

# **The Effect of Structural Changes on the Self-assembly of Novel Green Pyridinium-Carboxylate Gemini Surfactants in Langmuir and Langmuir-Blodgett Films**

Ala'a F. Eftaiha,<sup>a,b\*</sup> Abdussalam K. Qaroush,<sup>c\*</sup> Dina M. Foudeh,<sup>c</sup> Ahmad S. Abo-shunnar,<sup>a</sup> Suhad B. Hammad,<sup>c</sup> Khaleel I. Assaf,<sup>d</sup> and Matthew F. Paige<sup>e</sup>

<sup>a</sup> Department of Chemistry, Faculty of Science, The Hashemite University, Zarqa 13133, Jordan

<sup>b</sup> Department of Physics, Virginia Tech, Blacksburg, VA 24061, USA

<sup>c</sup> Department of Chemistry, Faculty of Science, The University of Jordan, Amman 11942, Jordan

<sup>d</sup> Department of Chemistry, Faculty of Science, Al-Balqa Applied University, Al-Salt 19117, Jordan

<sup>e</sup> Department of Chemistry, University of Saskatchewan, Saskatoon, SK S7N 5C9, Canada

## **Electronic Supplementary Information (ESI)**

# Table of Contents

List of Schemes.....	S3
List of Figures.....	S4
List of Tables .....	S6
1. Instruments.....	S7
2. Chemicals.....	S7
3. Synthesis and Characterization .....	S8
3.1 Pyridinium-Based Ester-Tethered GSs (12-14).....	S8
3.1.1 Activation of Py-n-CO <sub>2</sub> H and Synthesis of their Corresponding Structural Esters (Py-n-CO <sub>2</sub> C <sub>16</sub> ) (8-10).....	S8
3.1.2 Synthesis of PAGES, NAGS1, and INAGS (12-14) .....	S16
3.2 Pyridinium-Based Ester-Bonded Core GS (NAGS2).....	S23
3.2.1 Synthesis of <i>p</i> X-(OC(O)-3-Py) <sub>2</sub> , (1,4-phenylenebis(methylene) dinicotinate, 16) .....	S23
3.2.2 Synthesis of NAGS2 (3,3'-(((1,4-phenylenebis(methylene))bis(oxy))bis(carbonyl))bis(1-hexadecylpyridin-1-ium)•2Br .....	S26
4. Summary of Spectral Data.....	S29
5. References.....	S29

## List of Schemes

<b>Scheme S1.</b> Schematic representation for the synthesis of pyridinium-based ester-tethered GSs: (12) PAGES, (13) NAGS1 and (14) INAGS.....	S8
<b>Scheme S2.</b> The synthesis of <b>Py-n-CO<sub>2</sub>K (4-6)</b> and <b>Py-2-n-CO<sub>2</sub>C<sub>16</sub> (8-10)</b> .....	S9
<b>Scheme S3.</b> The synthesis of PAGES (12), NAGS1 (13), and INAGS (14).....	S17
<b>Scheme S4.</b> The synthesis of (16) <i>pX</i> -(OC(O)-3-Py) <sub>2</sub> .....	S24
<b>Scheme S5.</b> The synthesis of (17) NAGS2 .....	S27

## List of Figures

<b>Figure S1.</b> ATR-FTIR spectra of <b>Py-2-CO<sub>2</sub>H</b> (blue trace) and <b>Py-2-CO<sub>2</sub>C<sub>16</sub></b> (red trace).....	S10
<b>Figure S2.</b> <sup>1</sup> H NMR spectra of <b>Py-2-CO<sub>2</sub>H</b> (blue trace, S <sub>1</sub> : DMSO- <i>d</i> <sub>6</sub> ) and <b>Py-2-CO<sub>2</sub>C<sub>16</sub></b> (red trace, S <sub>2</sub> : CDCl <sub>3</sub> ). .....	S11
<b>Figure S3.</b> <sup>13</sup> C NMR spectra of <b>Py-2-CO<sub>2</sub>H</b> (blue trace, S <sub>1</sub> : DMSO- <i>d</i> <sub>6</sub> ) and <b>Py-2-CO<sub>2</sub>C<sub>16</sub></b> (red trace, S <sub>2</sub> : (CDCl <sub>3</sub> ))......	S11
<b>Figure S4.</b> ATR-FTIR spectra of <b>Py-3-CO<sub>2</sub>H</b> (blue trace) and <b>Py-3-CO<sub>2</sub>C<sub>16</sub></b> (red trace).....	S12
<b>Figure S5.</b> <sup>1</sup> H NMR spectra of <b>Py-3-CO<sub>2</sub>H</b> (blue trace, S <sub>1</sub> : DMSO- <i>d</i> <sub>6</sub> ) and <b>Py-3-CO<sub>2</sub>C<sub>16</sub></b> (red trace, S <sub>2</sub> : CDCl <sub>3</sub> ). .....	S13
<b>Figure S6.</b> <sup>13</sup> C NMR spectra of <b>Py-3-CO<sub>2</sub>H</b> (blue trace, S <sub>1</sub> : DMSO- <i>d</i> <sub>6</sub> ) and <b>Py-3-CO<sub>2</sub>C<sub>16</sub></b> (red trace, S <sub>2</sub> : CDCl <sub>3</sub> ). .....	S14
<b>Figure S7.</b> ATR-FTIR spectra of <b>Py-4-CO<sub>2</sub>H</b> (blue trace) and <b>Py-4-CO<sub>2</sub>C<sub>16</sub></b> (red trace). The peak centered at the wavenumber of 3676 cm <sup>-1</sup> corresponding to water presence in the sample. ....	S15
<b>Figure S8.</b> <sup>1</sup> H NMR spectra of <b>Py-4-CO<sub>2</sub>H</b> (blue trace, S <sub>1</sub> : DMSO- <i>d</i> <sub>6</sub> , S <sub>2</sub> : DMF- <i>d</i> <sub>7</sub> ) and <b>Py-4-CO<sub>2</sub>C<sub>16</sub></b> (red trace, S <sub>3</sub> : CDCl <sub>3</sub> , X: DMSO).....	S15
<b>Figure S9.</b> <sup>13</sup> C NMR spectra of <b>Py-4-CO<sub>2</sub>H</b> (blue trace, S <sub>1</sub> : DMSO- <i>d</i> <sub>6</sub> , S <sub>2</sub> : DMF- <i>d</i> <sub>7</sub> ) and <b>Py-4-CO<sub>2</sub>C<sub>16</sub></b> (red trace, S <sub>3</sub> : CDCl <sub>3</sub> , X: DMSO).....	S16
<b>Figure S10.</b> ATR-FTIR spectra of <b>Py-2-CO<sub>2</sub>C<sub>16</sub></b> (blue trace) and <b>PAGS</b> (red trace). .....	S18
<b>Figure S11.</b> <sup>1</sup> H NMR spectra of <b>Py-2-CO<sub>2</sub>C<sub>16</sub></b> (blue trace) and <b>PAGS</b> (red trace) (S: CDCl <sub>3</sub> ). S18	
<b>Figure S12.</b> <sup>13</sup> C NMR spectra of <b>Py-2-CO<sub>2</sub>C<sub>16</sub></b> (blue trace) and <b>PAGS</b> (red trace) (S: CDCl <sub>3</sub> ). S19	
<b>Figure S13.</b> ATR-FTIR spectra of <b>Py-3-CO<sub>2</sub>C<sub>16</sub></b> (blue trace) and <b>NAGS1</b> (red trace).....	S20
<b>Figure S14.</b> <sup>1</sup> H NMR spectra of <b>Py-3-CO<sub>2</sub>C<sub>16</sub></b> (blue trace) and <b>NAGS1</b> (red trace) (S: CDCl <sub>3</sub> ). .....	S20

<b>Figure S15.</b> $^{13}\text{C}$ NMR spectra of <b>Py-3-CO<sub>2</sub>C<sub>16</sub></b> (blue trace) and NAGS1 (red trace) (S: CDCl <sub>3</sub> ).	S21
<b>Figure S16.</b> ATR-FTIR spectra of <b>Py-4-CO<sub>2</sub>C<sub>16</sub></b> (blue trace) and INAGS (red trace).	S22
<b>Figure S17.</b> $^1\text{H}$ NMR spectra of <b>Py-4-CO<sub>2</sub>C<sub>16</sub></b> (blue trace) and INAGS (red trace) (S: CDCl <sub>3</sub> , X: DMSO).	S22
<b>Figure S18.</b> $^{13}\text{C}$ NMR spectra of <b>Py-4-CO<sub>2</sub>C<sub>16</sub></b> (blue trace) and INAGS (red trace) (S <sub>1</sub> : CDCl <sub>3</sub> , S <sub>2</sub> : CD <sub>3</sub> OD, X: DMSO).	S23
<b>Figure S19.</b> ATR-FTIR spectra of <b>Py-3-CO<sub>2</sub>H (2, blue trace), 15 (red trace), and pX-(OC(O)-3-Py)<sub>2</sub> (16, green trace)</b> .	S25
<b>Figure S20.</b> $^1\text{H}$ NMR spectra of <b>Py-3-CO<sub>2</sub>H (2, blue trace), 15 (red trace), and pX-(OC(O)-3-Py)<sub>2</sub> (16, green trace)</b> (S <sub>1</sub> : DMSO- <i>d</i> <sub>6</sub> , S <sub>2</sub> : CDCl <sub>3</sub> , X <sub>1</sub> : H <sub>2</sub> O, X <sub>2</sub> : EtOH).	S25
<b>Figure S21.</b> $^{13}\text{C}$ NMR spectra of <b>Py-3-CO<sub>2</sub>H (2, blue trace), 15 (red trace), and pX-(OC(O)-3-Py)<sub>2</sub> (16, green trace)</b> (S <sub>1</sub> : DMSO- <i>d</i> <sub>6</sub> , S <sub>2</sub> : CDCl <sub>3</sub> ).	S26
<b>Figure S22.</b> ATR-FTIR spectra of <b>pX-(OC(O)-3-Py)<sub>2</sub> (16, blue trace), and NAGS2 (15, red trace)</b> .	S27
<b>Figure S23.</b> $^1\text{H}$ NMR spectra of <b>pX-(OC(O)-3-Py)<sub>2</sub> (16, blue trace), and NAGS2 (15, red trace)</b> (S <sub>1</sub> : CDCl <sub>3</sub> , S <sub>2</sub> : CD <sub>3</sub> OD, X: EtOH).	S28
<b>Figure S24.</b> $^{13}\text{C}$ NMR spectra of <b>pX-(OC(O)-3-Py)<sub>2</sub> (16, blue trace), and NAGS2 (15, red trace)</b> (S <sub>1</sub> : CDCl <sub>3</sub> , S <sub>2</sub> : CD <sub>3</sub> OD, X: EtOH).	S28

## List of Tables

<b>Table S1.</b> $^1\text{H}$ NMR chemical shifts ( $\delta$ , ppm) of the synthesized GSs.....	S29
<b>Table S2.</b> $^{13}\text{C}$ NMR chemical shifts ( $\delta$ , ppm) of the synthesized GSs.....	S30
<b>Table S3.</b> ATR-FTIR wavenumbers ( $\tilde{\nu}$ , $\text{cm}^{-1}$ ) of the synthesized GSs.....	S31

## 1. Instruments

$^1\text{H}$  and  $^{13}\text{C}$  nuclear magnetic resonance (NMR) solution spectra were collected at ambient temperature using a Bruker 500 MHz AVANCE-III NMR ( $^1\text{H}$ : 500 MHz and  $^{13}\text{C}$ : 125 MHz) (Bruker, Switzerland). *Ex situ* ATR-FTIR spectra were recorded using Bruker Vertex 70-FT-IR spectra at room temperature coupled with a Vertex Pt-ATR-FTIR accessory (Bruker, Switzerland). Elemental analysis was completed by an EA3000 (Eurovector, Italy). While the corrected melting point was measured using a Cole-Palmer MP-400D, (Stuart, United Kingdom) high-temperature, high-resolution digital melting point apparatus; 115/230 VAC, temperature accuracy  $\pm 0.5$  °C.

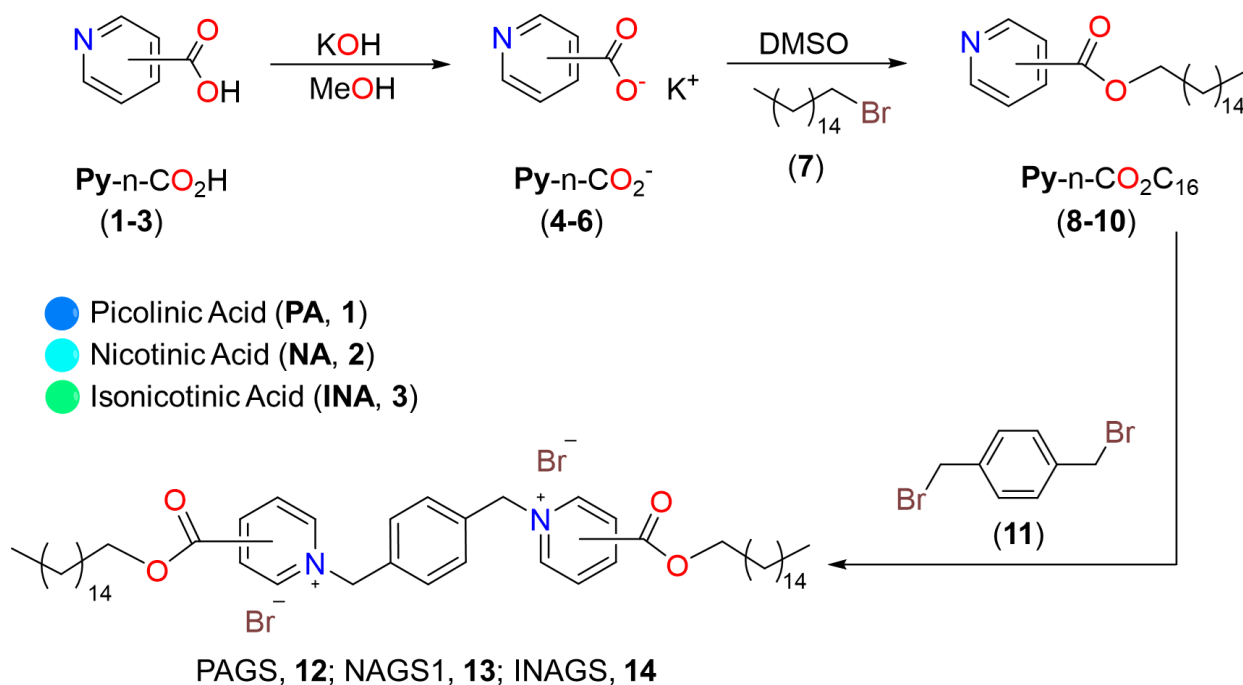
## 2. Chemicals

Picolinic acid (99%), isonicotinic acid (99%) 1-bromohexadecane (97%), 2-chloro-1-methylpyridinium iodide (97%), acetonitrile (HPLC-grade), and dimethyl sulfoxide- $d_6$  (DMSO- $d_6$ , 99.5% atom D), were obtained from Sigma Aldrich.  $\alpha,\alpha'$ -dibromo-*p*-xylene (97%), dimethylformamide- $d_7$  (DMF- $d_7$ , 99.5% atom D), and chloroform- $d$  ( $\text{CHCl}_3$ - $d$ , 99.8% atom D) were purchased from Acros Organics. Nicotinic acid (98%) and methyl- $d_3$  alcohol- $d$  (MeOH- $d_4$ , 99.5% atom D), were purchased from Janseen Chimica. 1,4-benzenedimethanol (99%) and dipalmitoylphosphatidylcholine (99%) were purchased from TCI and Avanti polar lipids, respectively. Potassium hydroxide (KOH), methanol (MeOH, AR-grade), hexane (HPLC-grade), were purchased from LAB CHEM. Chloroform ( $\text{CHCl}_3$ , HPLC-grade), and sodium sulfate anhydrous were obtained from Carlo Erba reagents. Triethylamine (AR-grade), toluene (HPLC-grade) and DMSO (HPLC-grade), were purchased from Fischer, Macron fine chemicals, and TEDIA, respectively. Dichloromethane (99.95%) and isopropanol were purchased from ChemPure and distilled from a suspension of anhydrous sodium sulfate.

### 3. Synthesis and Characterization

#### 3.1 Pyridinium-Based Ester-Tethered GSs (12-14)

The synthesis of GSs (**12-14**) was carried out with a slight modification in the reaction conditions compared to the previously published procedures by our research group,<sup>1</sup> as shown in **Scheme S1**. Pyridine-*n*-carboxylic acids (**Py-n-CO<sub>2</sub>H**; *n* = 2, 3, 4) starting materials (**1-3**) were activated with methanolic KOH, followed by the reaction with 1-bromohexadecane (**7**) to yield pyridine-based esters (**8-10**). Then, the latter compounds were reacted with  $\alpha,\alpha'$ -dibromo-*p*-xylene (**11**) to give the GSs (**12-14**).



**Scheme S1.** Schematic representation for the synthesis of pyridinium-based ester-tethered GSs: (**12**) PAGS, (**13**) NAGS1 and (**14**) INAGS.

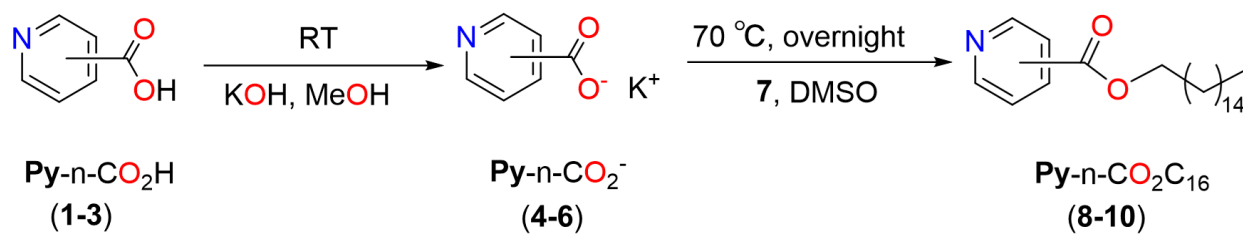
##### 3.1.1 Activation of **Py-n-CO<sub>2</sub>H** and Synthesis of their Corresponding Structural Esters (**Py-n-CO<sub>2</sub>C<sub>16</sub>**) (**8-10**)

As shown in **Scheme S2**, suspensions of **Py-n-CO<sub>2</sub>H** (**1-3**, 5.0 g, 1 eq.) in sufficient amounts of MeOH were prepared. Afterwards, proper amount of methanolic potassium hydroxide (1.2 eq.)



was added. The mixtures were stirred until the salt adducts were fully dissolved. Subsequently, appropriate amounts of isopropanol were added to precipitate compounds **4-6**, then the precipitates were collected using suction filtration, twice washed with diethyl ether ( $2 \times 25$  mL), and dried over air.

1.0 g (6.20 mmol) of the salt adducts were dissolved in 20, 50, and 30 mL of DMSO at 110 °C for **5**, **4**, **6**, respectively. Afterwards, the hot solutions were left to cool down to 70 °C to prevent any side reactions, followed by a dropwise addition of a 2 mL toluene solution of 1-bromohexadecane (1.81 g, 6.20 mmol, **7**), and left to stir overnight at the same temperature. Subsequently, the reactions were cooled down to room temperature (RT), then extracted with ( $2 \times 50$  mL) of hexane, which was evaporated to form solid precipitates. For further treatment and purification, quantitative transfer of the former precipitates into separate beakers, each was stirred in 75 mL of acetonitrile and left to soak for 1 h, then the precipitates were collected using suction filtration and dried over air. **Py-2-CO<sub>2</sub>C<sub>16</sub>** (Color: off white; Yield: 52%), **Py-3-CO<sub>2</sub>C<sub>16</sub>** (Color: off white; Yield: 59%), and **Py-4-CO<sub>2</sub>C<sub>16</sub>** (Color: white; Yield: 84%).



**Scheme S2.** The synthesis of **Py-n-CO<sub>2</sub>K** (**4-6**) and **Py-2-n-CO<sub>2</sub>C<sub>16</sub>** (**8-10**).

Structures **8-10** were examined using ATR-FTIR spectroscopy (**Figure S1**, **Figure S4**, and **Figure S7**, red traces), where the stretching frequencies at 1733, 1718, and 1722  $\text{cm}^{-1}$  corresponding to the newly formed ester groups appeared.<sup>2</sup> The tethering of the aliphatic tail was further confirmed by the appearance of new peaks ranging from 2830 to 2940  $\text{cm}^{-1}$ . Furthermore, <sup>1</sup>H and <sup>13</sup>C NMR spectra confirmed the formation of **8-10** in which new peaks that are corresponded to the

methylene moiety closest to the ester functional groups emerged within 4.33-4.40 ppm (c, **Figure S2**, **Figure S5**, and **Figure S8**, red traces) and 65.7-66.3 ppm (c, **Figure S3**, **Figure S6**, and **Figure S9**, red traces).<sup>3</sup>

For **Py-2-CO<sub>2</sub>C<sub>16</sub>**, m.p. (corrected) = 53 °C; <sup>1</sup>H NMR (500 MHz, CHCl<sub>3</sub>-d): δ (ppm) = 8.75 (1 H, d), 8.10 (1 H, d), 7.83 (1 H, t), 7.46 (1 H, t), 4.40 (4 H, t), 1.42 (4 H, p), 1.24 (22 H, m), 0.86 (3 H, t); <sup>13</sup>C NMR (125 MHz, CHCl<sub>3</sub>-d): δ (ppm) = 165.3, 149.9, 148.3, 137.0, 126.8, 125.1, 66.1, 32.0, 29.7, 29.7, 29.6, 29.6, 29.5, 29.4, 29.3, 28.7, 25.9, 22.7, 14.12; **ATR-FTIR**:  $\tilde{\nu}$  (cm<sup>-1</sup>) = 2956, 2935, 2836, 1733, 1579, 1471, 1243, 1135, 748. **Elemental analysis** (C<sub>22</sub>H<sub>37</sub>NO<sub>2</sub>); calculated (%) C, 76.03; H, 10.73; N, 4.03; found (%) C, 76.07; H, 10.92; N, 4.07.

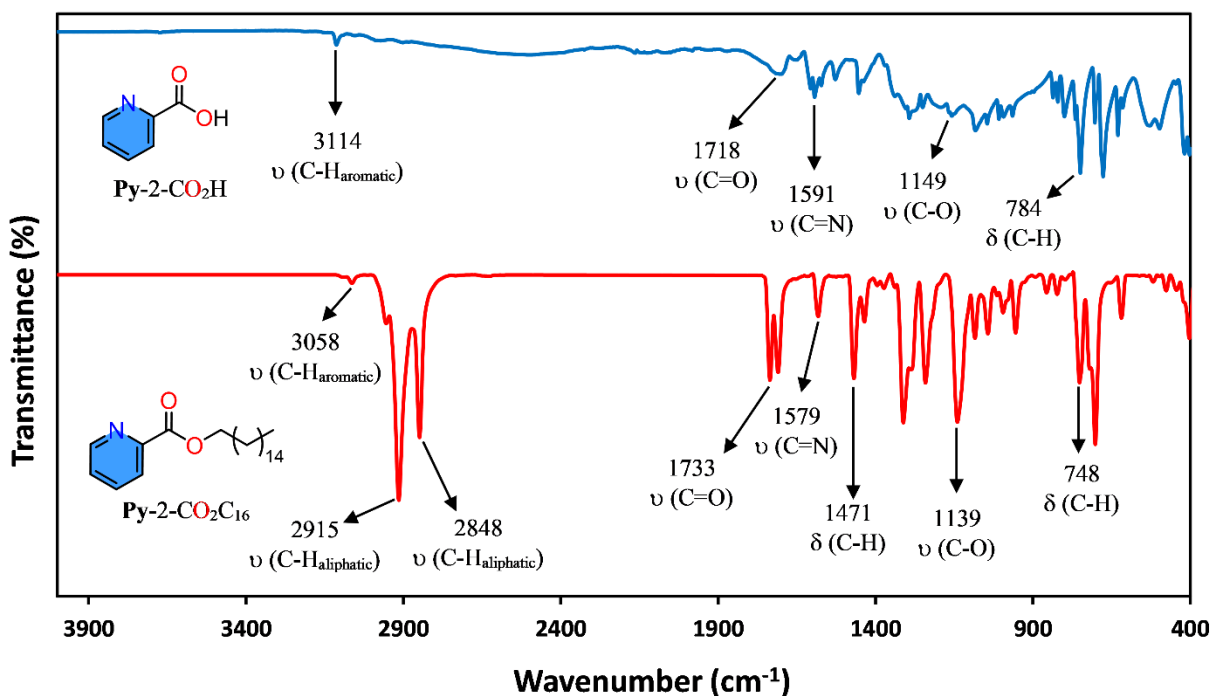


**Figure S1.** ATR-FTIR spectra of **Py-2-CO<sub>2</sub>H** (blue trace) and **Py-2-CO<sub>2</sub>C<sub>16</sub>** (red trace).

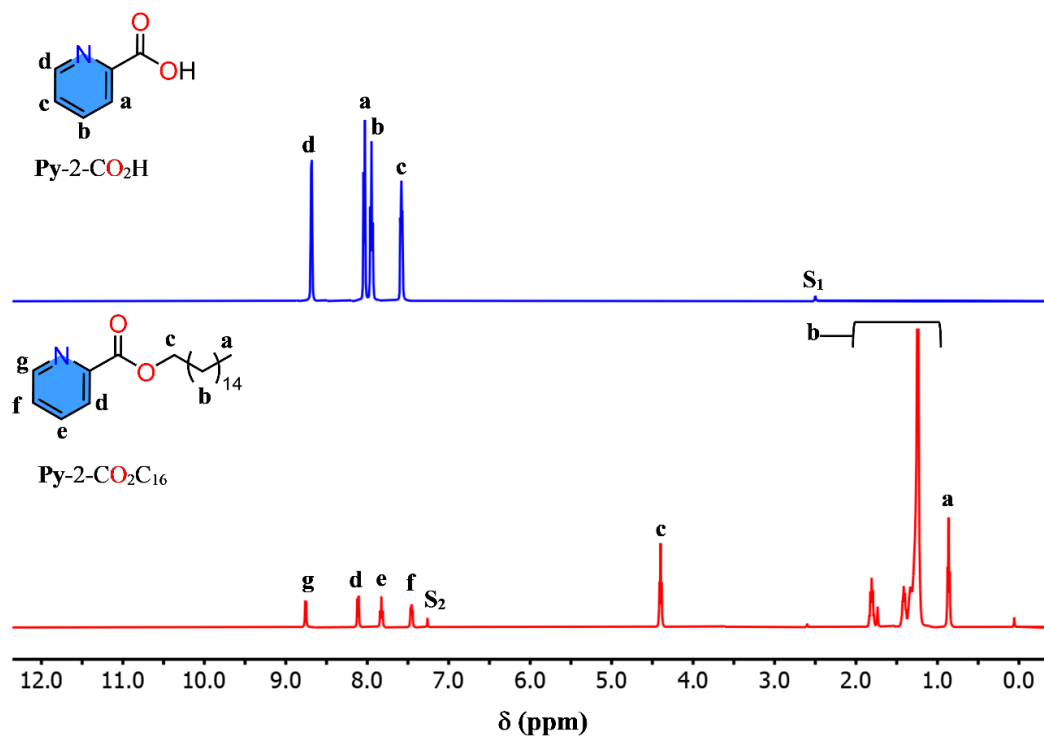


**Figure S2.**  $^1\text{H}$  NMR spectra of **Py-2-CO<sub>2</sub>H** (blue trace, S<sub>1</sub>: DMSO-*d*<sub>6</sub>) and **Py-2-CO<sub>2</sub>C<sub>16</sub>** (red trace, S<sub>2</sub>: CDCl<sub>3</sub>).

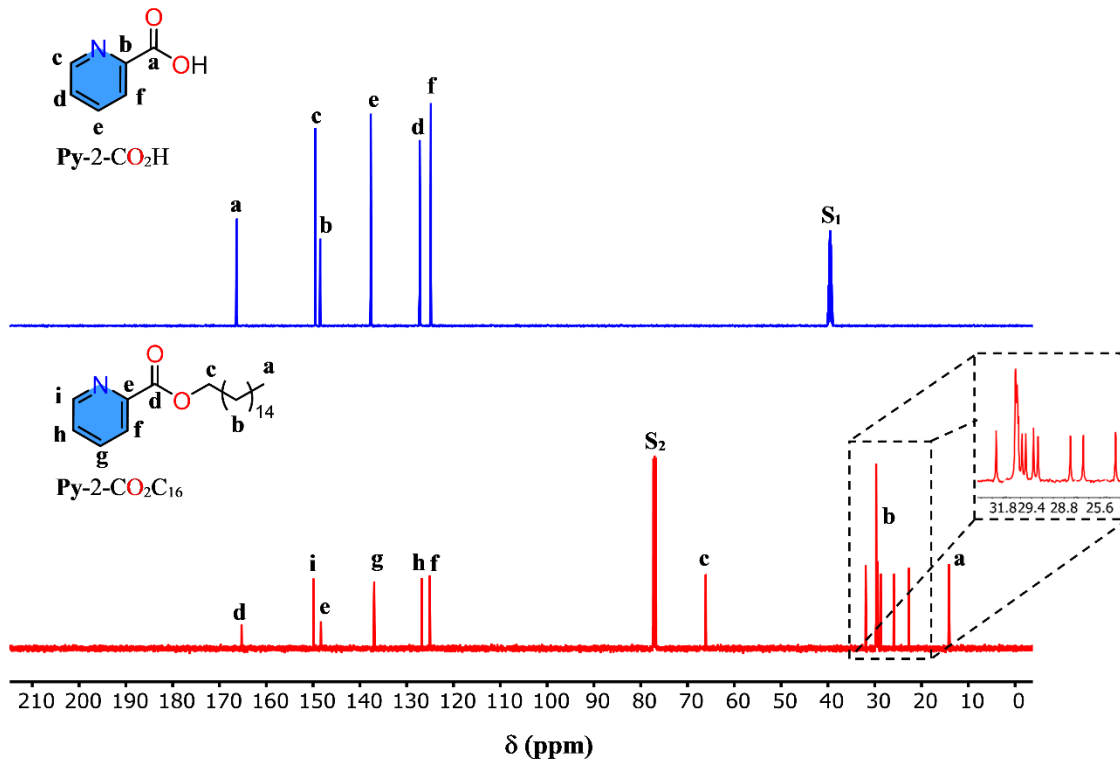


**Figure S3.**  $^{13}\text{C}$  NMR spectra of **Py-2-CO<sub>2</sub>H** (blue trace, S<sub>1</sub>: DMSO-*d*<sub>6</sub>) and **Py-2-CO<sub>2</sub>C<sub>16</sub>** (red trace, S<sub>2</sub>: CDCl<sub>3</sub>).

For **Py-3-CO<sub>2</sub>C<sub>16</sub>**, m.p. (corrected) = 51 °C. **<sup>1</sup>H NMR** (500 MHz, CDCl<sub>3</sub>): δ (ppm) = 9.21 (1 H, s), 8.76 (1 H, d), 7.37 (1 H, t), 4.33 (4 H, t), 1.78 (4 H, p), 1.42 (4 H, p), 1.24 (18 H, m), 0.86 (3 H, t); **<sup>13</sup>C NMR** (125 MHz, CDCl<sub>3</sub>): δ (ppm) = 165.4, 153.4, 151.0, 137.1, 126.5, 123.5, 65.7, 32.0, 29.8, 29.8, 29.7, 29.6, 29.5, 29.4, 28.8, 26.1, 22.8, 14.2; **ATR-FTIR**:  $\tilde{\nu}$  (cm<sup>-1</sup>) = 2931, 2915, 2850, 1718, 1592, 1472, 1424, 1292, 1129, 740, 699; **Elemental analysis** (C<sub>22</sub>H<sub>37</sub>NO<sub>2</sub>); calculated (%): C, 76.03; H, 10.73; N, 4.03; found (%): C, 75.98; H, 10.72; N, 4.14.

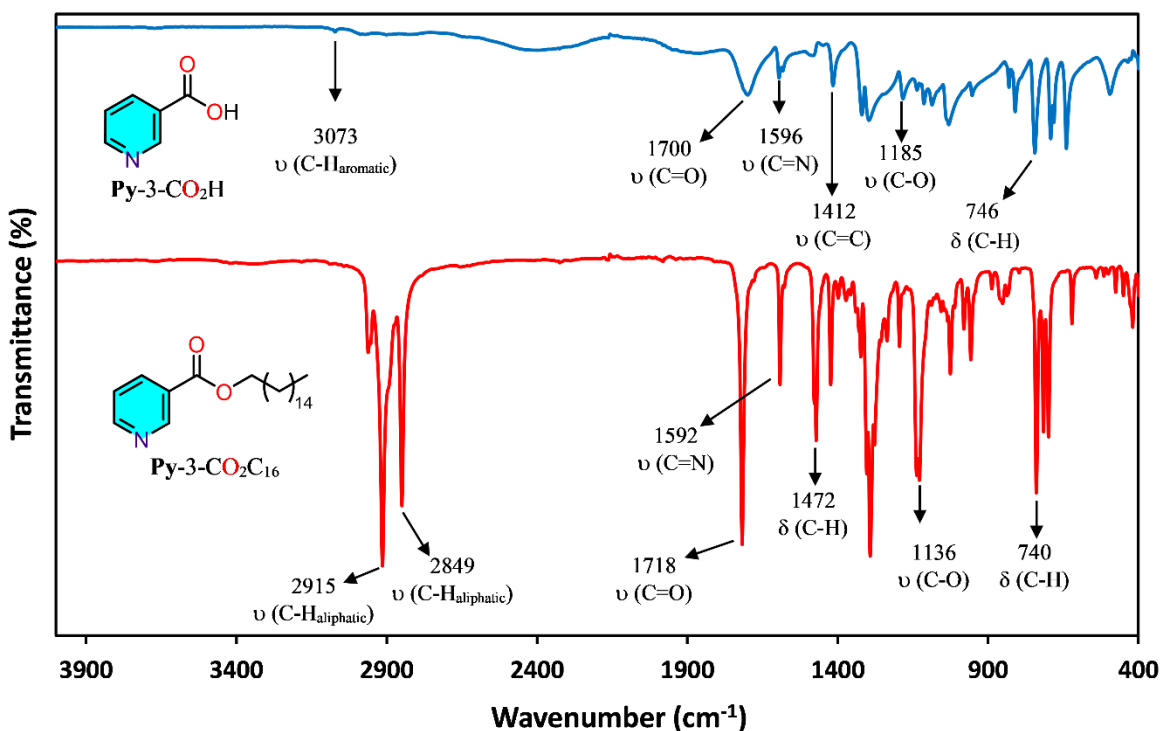


**Figure S4.** ATR-FTIR spectra of **Py-3-CO<sub>2</sub>H** (blue trace) and **Py-3-CO<sub>2</sub>C<sub>16</sub>** (red trace).

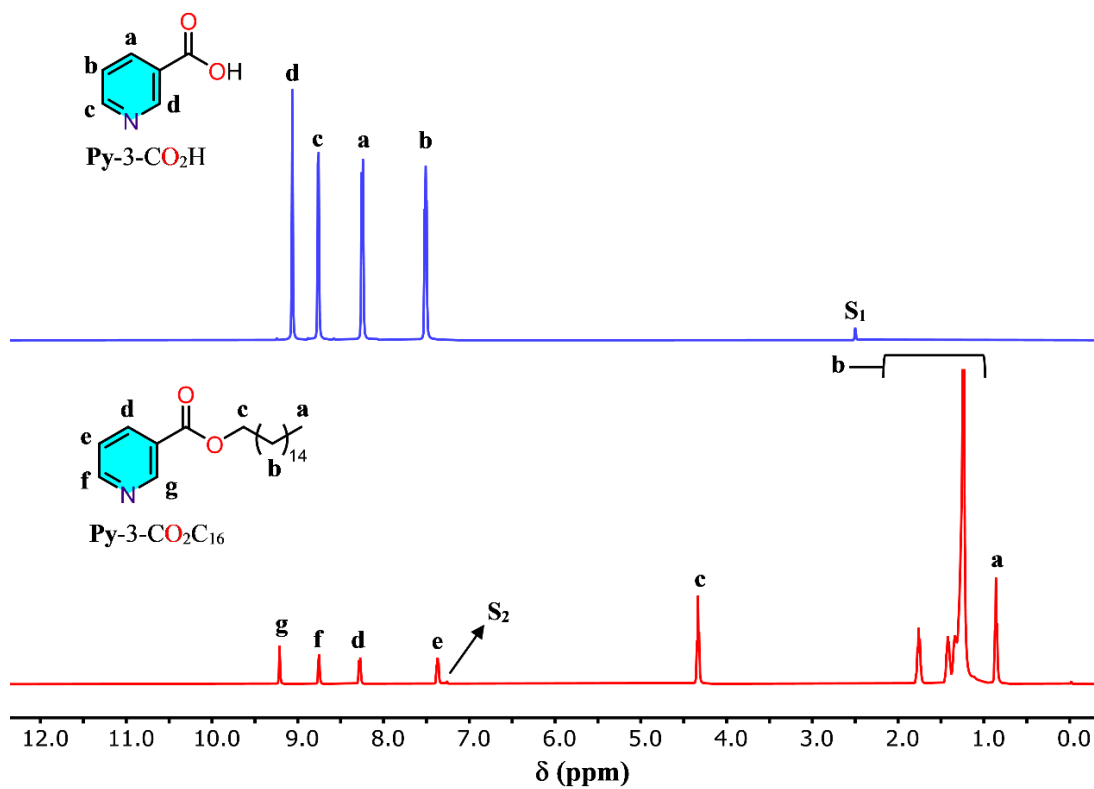


**Figure S5.** <sup>1</sup>H NMR spectra of **Py-3-CO<sub>2</sub>H** (blue trace, S<sub>1</sub>: DMSO-*d*<sub>6</sub>) and **Py-3-CO<sub>2</sub>C<sub>16</sub>** (red trace, S<sub>2</sub>: CDCl<sub>3</sub>).

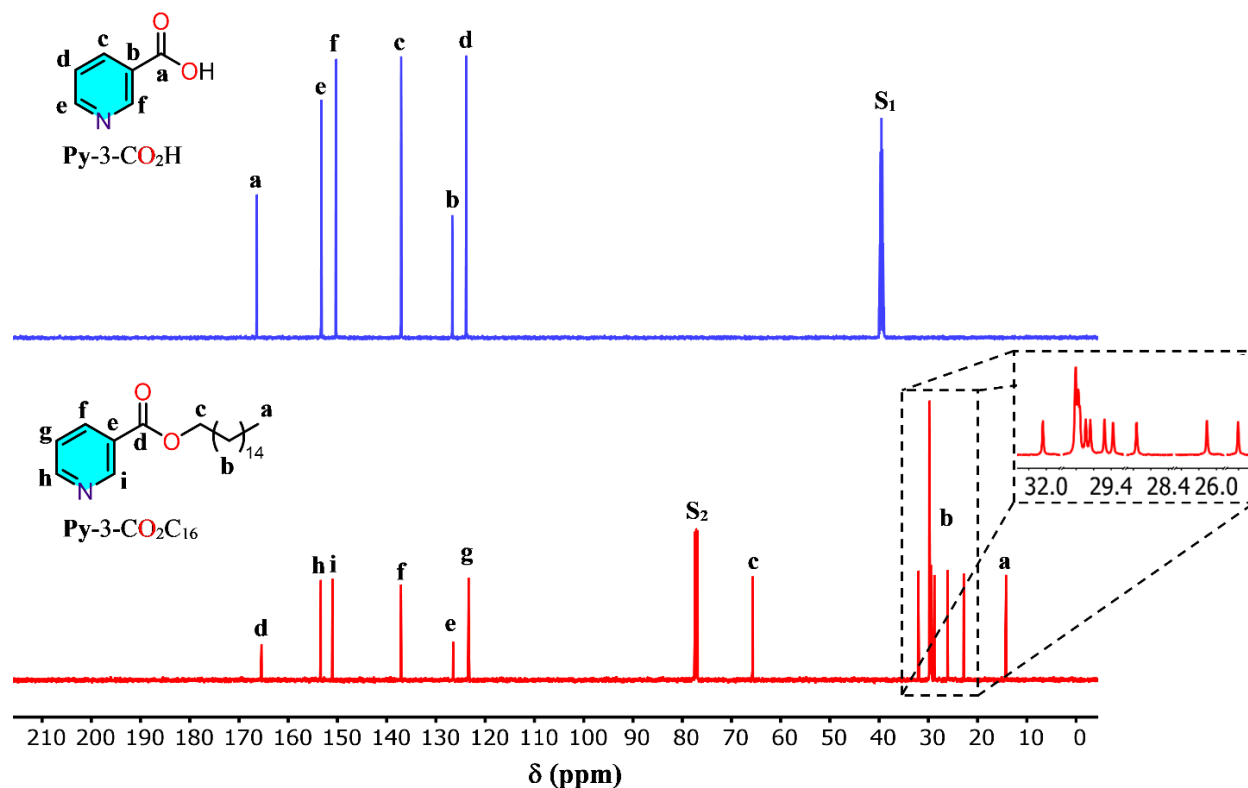


**Figure S6.**  $^{13}\text{C}$  NMR spectra of Py-3-CO<sub>2</sub>H (blue trace, S<sub>1</sub>: DMSO-*d*<sub>6</sub>) and Py-3-CO<sub>2</sub>C<sub>16</sub> (red trace, S<sub>2</sub>: CDCl<sub>3</sub>).

For Py-4-CO<sub>2</sub>C<sub>16</sub>, m.p. (corrected) = 53 °C.  $^1\text{H}$  NMR (500 MHz, CDCl<sub>3</sub>):  $\delta$  (ppm) = 8.79 (2 H, d), 7.87 (2 H, d), 4.35 (2 H, t), 1.76 (2 H, p), 1.43 (2 H, p), 1.25 (24 H, m), 0.87 (3 H, t).  $^{13}\text{C}$  NMR (125 MHz, CDCl<sub>3</sub>):  $\delta$  (ppm) = 165.1, 150.2, 138.4, 123.2, 66.3, 32.1, 29.8, 29.8, 29.7, 29.6, 29.5, 29.4, 28.7, 26.1, 22.8, 14.2; ATR-FTIR:  $\tilde{\nu}$  (cm<sup>-1</sup>) = 2960, 2914, 2848, 1560, 1722, 1471, 1286, 1135, 751. **Elemental analysis** (C<sub>22</sub>H<sub>37</sub>NO<sub>2</sub>); calculated (%) C, 76.03; H, 10.73; N, 4.03; found (%) C, 75.83; H, 10.73; N, 4.11.

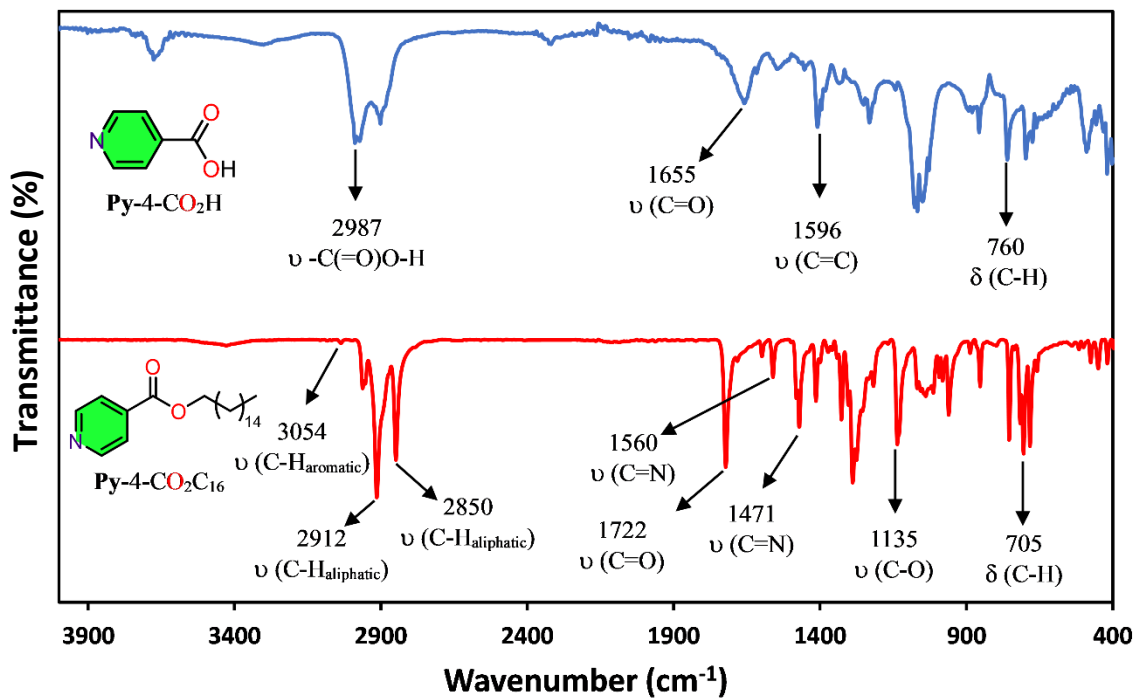


**Figure S7.** ATR-FTIR spectra of Py-4-CO<sub>2</sub>H (blue trace) and Py-4-CO<sub>2</sub>C<sub>16</sub> (red trace). The peak centered at the wavenumber of 3676 cm<sup>-1</sup> corresponding to water presence in the sample.

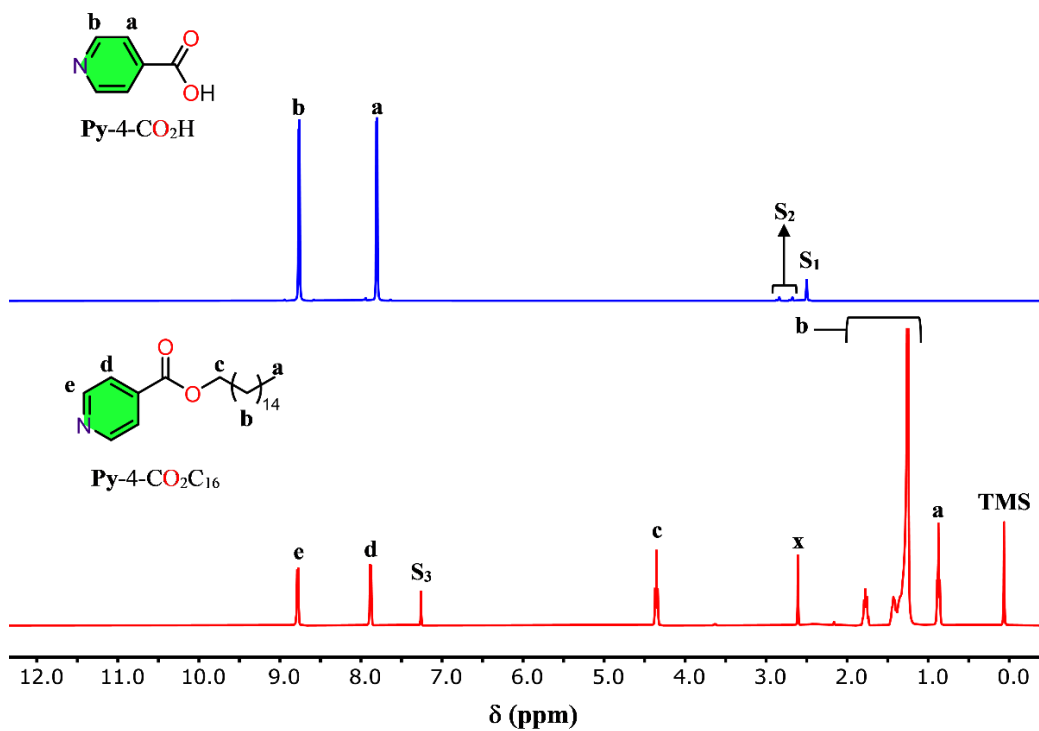


**Figure S8.** <sup>1</sup>H NMR spectra of Py-4-CO<sub>2</sub>H (blue trace, S<sub>1</sub>: DMSO-*d*<sub>6</sub>, S<sub>2</sub>: DMF-*d*<sub>7</sub>) and Py-4-CO<sub>2</sub>C<sub>16</sub> (red trace, S<sub>3</sub>: CDCl<sub>3</sub>, X: DMSO)

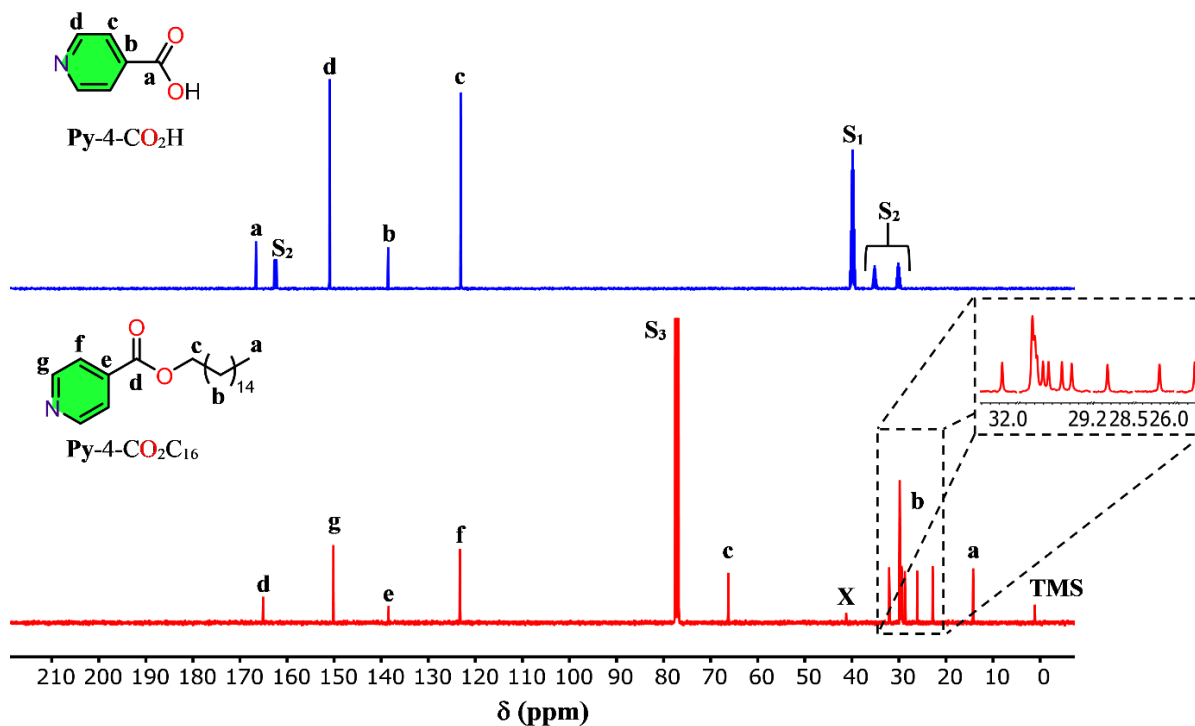
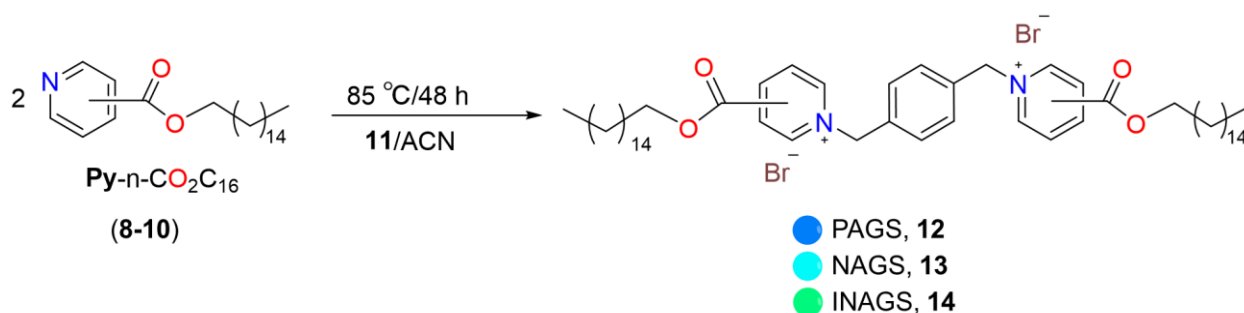


**Figure S9.**  $^{13}\text{C}$  NMR spectra of **Py-4-CO<sub>2</sub>H** (blue trace, S<sub>1</sub>: DMSO-*d*<sub>6</sub>, S<sub>2</sub>: DMF-*d*<sub>7</sub>) and **Py-4-CO<sub>2</sub>C<sub>16</sub>** (red trace, S<sub>3</sub>: CDCl<sub>3</sub>, X: DMSO)

### 3.1.2 Synthesis of PAGS, NAGS1, and INAGS (12-14)

Solutions of **Py-n-CO<sub>2</sub>C<sub>16</sub>** (**8-10**, 1.0 g, 2.2 eq.) in proper amounts of freshly distilled acetonitrile (ACN) were charged into one-necked round bottom flasks equipped with reflux condensers and rubber septa, followed by a dropwise addition of 15 mL of freshly distilled ACN solution of  $\alpha,\alpha'$ -dibromo-*p*-xylene (**11**, 1 eq.). The reaction mixtures were refluxed for 48 h at 85 °C (**Scheme S3**). At the end of the reactions, solvents were evaporated, and the crude precipitates were recrystallized from chloroform/diethyl ether (3/10; v/v) mixture. The desired products (**12-14**) were collected using suction filtration and dried over air. PAGS (Color: white; Yield: 80%), NAGS1 (Color: off white; Yield: 87%), and INAGS (Color: yellow; Yield: 89%).





**Scheme S3.** The synthesis of PAGS (**12**), NAGS1 (**13**), and INAGS (**14**).

Structures **12-14** were examined using ATR-FTIR (**Figure S10**, **Figure S13**, and **Figure S16**, red traces). C=N stretching frequency shifted from 1583 to 1640, 1592 to 1636, and from 1560 to 1640  $\text{cm}^{-1}$  for PAGS, NAGS1, and INAGS, respectively, as a result of quaternization. In addition, C=C stretching peaks, related to *p*-xylene, appeared at 1594, 1593, and 1571 for PAGS, NAGS1, and INAGS, respectively.  $^1\text{H}$  NMR spectra showed the emergence of two new peaks ranging between 6.60-6.65 ppm and 7.80-7.87 ppm resembling the methylene and benzene ring moieties in the xylylene spacer group, respectively (**Figure S11**, **Figure S14**, and **Figure S17**, red traces). Furthermore,  $^{13}\text{C}$  NMR spectra confirm their presence in between 63.0-64.5 ppm, for the methylene moiety, and 129.2-131.2, 131.0-134.7 ppm for the benzene ring moiety in the spacer (**Figure S12**, **Figure S15**, and **Figure S18**, red traces).<sup>1</sup> It is noteworthy that the associated peaks present in the xylylene bromide (**11**) exhibited peaks at 4.56 together with 7.11 ppm as well as 33.3 and 129.3, and 138.2 ppm, which clearly showed the successful quaternization to give the GSs **12-14**.

For PAGS, m.p. (corrected) = 180 °C.  $^1\text{H}$  NMR (500 MHz,  $\text{CDCl}_3$ ):  $\delta$  (ppm) = 10.11 (2 H, d), 10.00 (2 H, s), 8.32 (2 H, t), 7.80 (4 H, s), 6.61 (4 H, s), 4.39 (4 H, t), 2.13 (4 H, p), 1.81 (4 H, p), 1.25 (50 H, m), 0.87 (6 H, t);  $^{13}\text{C}$  NMR (125 MHz,  $\text{CDCl}_3$ ):  $\delta$  (ppm) = 161.3, 149.1, 146.2, 145.3, 134.9, 131.4, 131.0, 129.2, 67.9, 63.3, 32.1, 29.9, 28.6, 26.0, 22.8, 14.2; ATR-FTIR:  $\tilde{\nu}$  ( $\text{cm}^{-1}$ ) = 2999, 2920, 2851, 1725, 1640, 1594, 1471, 1307, 744.

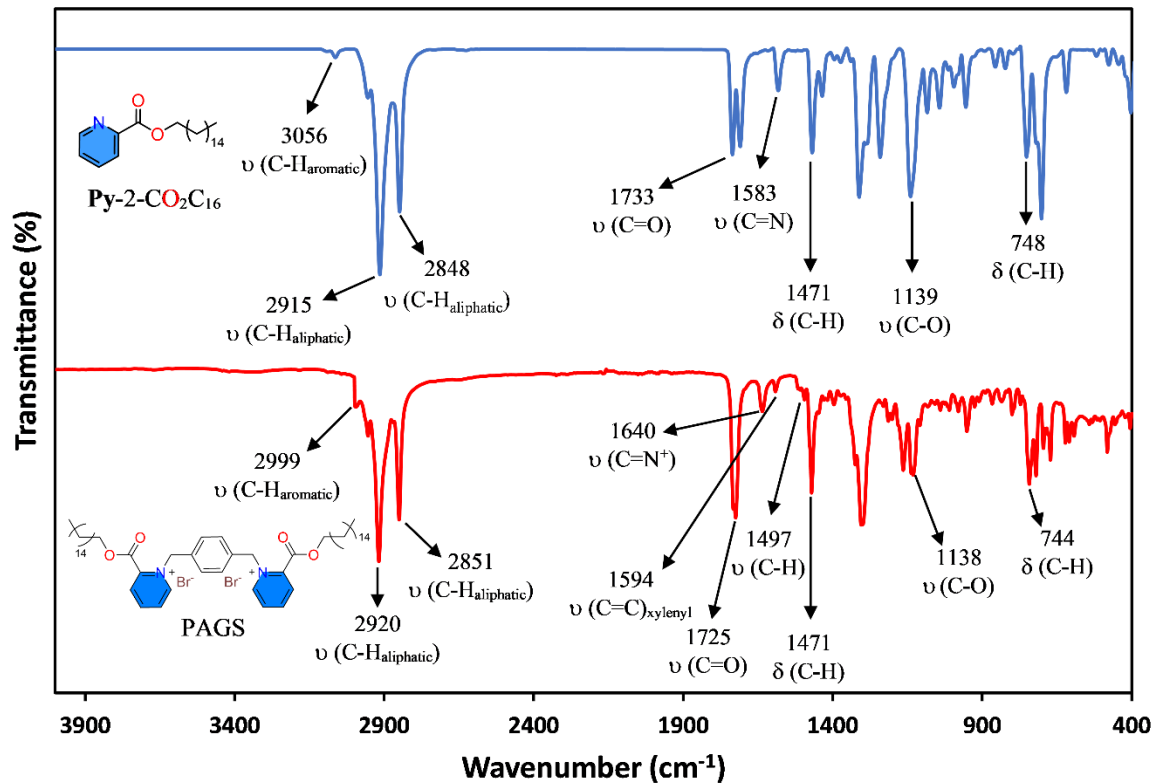


Figure S10. ATR-FTIR spectra of Py-2-CO<sub>2</sub>C<sub>16</sub> (blue trace) and PAPS (red trace).

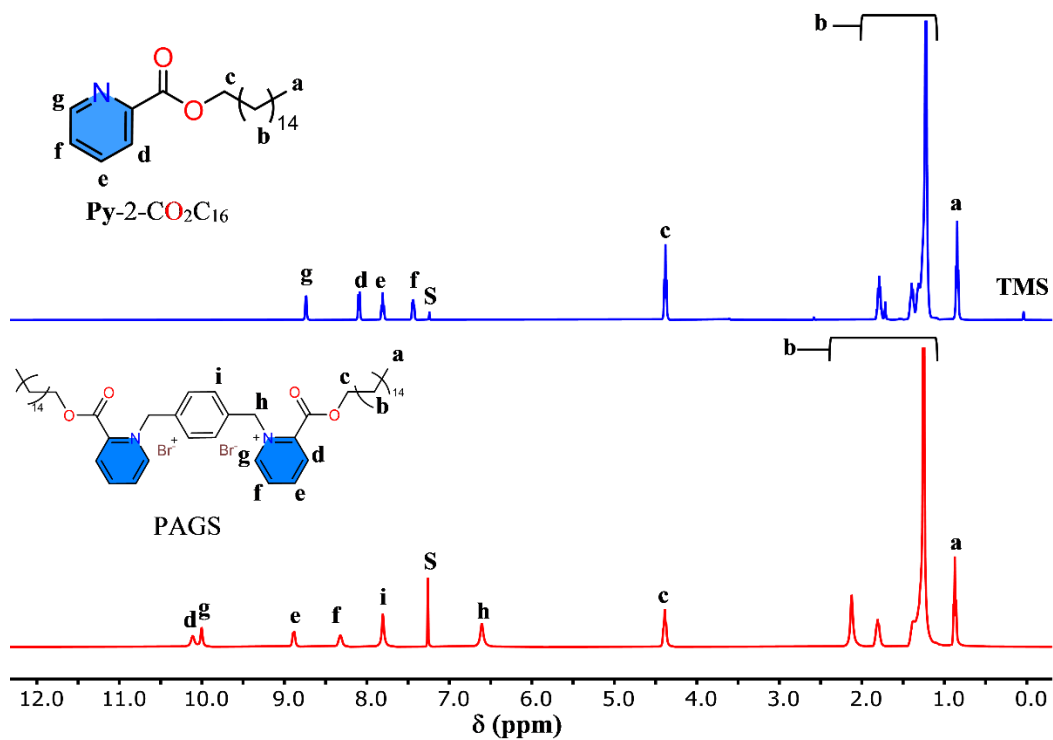
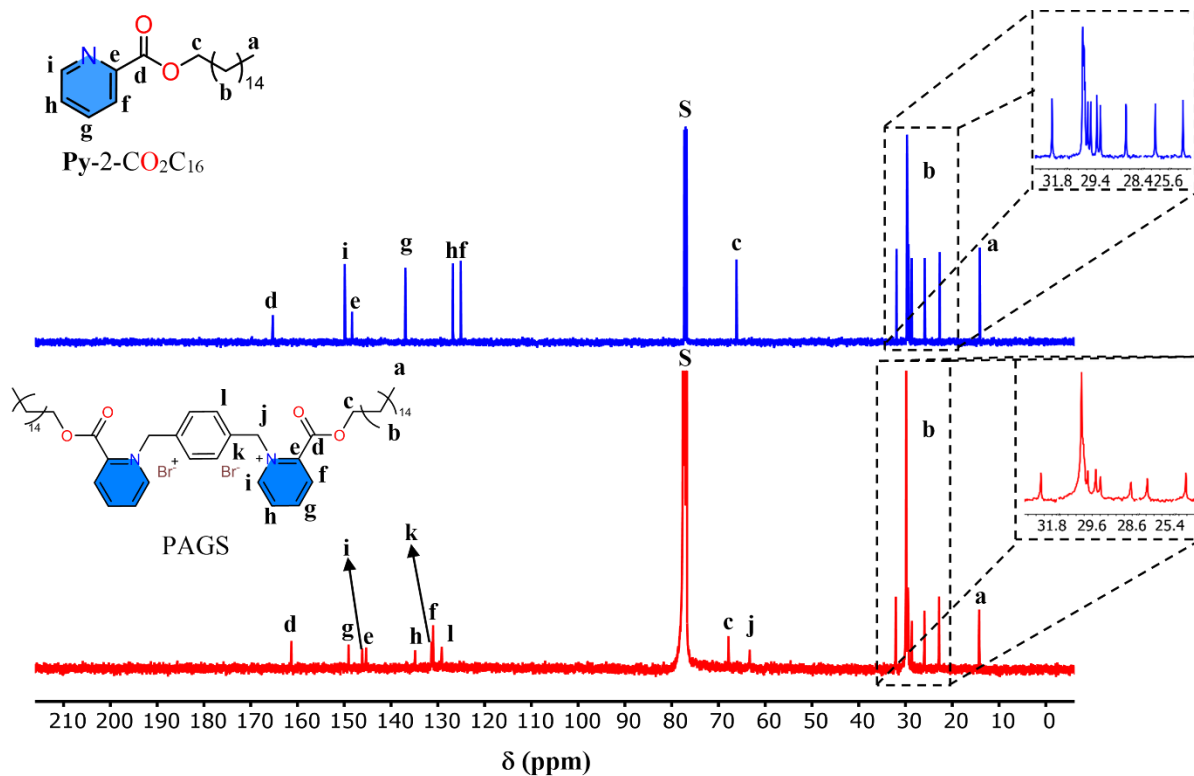


Figure S11. <sup>1</sup>H NMR spectra of Py-2-CO<sub>2</sub>C<sub>16</sub> (blue trace) and PAPS (red trace) (S: CDCl<sub>3</sub>).



**Figure S12.**  $^{13}\text{C}$  NMR spectra of **Py-2-CO<sub>2</sub>C<sub>16</sub>** (blue trace) and **PAGES** (red trace) (S:  $\text{CDCl}_3$ ).

For **NAGS1**, m.p. (corrected) = 189 °C.  $^1\text{H}$  NMR (500 MHz,  $\text{CDCl}_3$ ):  $\delta$  (ppm) = 10.09 (2 H, d), 10.02 (2 H, s), 8.87 (2 H, d), 8.35 (2 H, t), 7.80 (4 H, s), 6.60 (4 H, s), 4.38 (4 H, t), 2.20 (4 H, p), 1.81 (4 H, p), 1.24 (48 H, s), 0.88 (6 H, t);  $^{13}\text{C}$  NMR (125 MHz,  $\text{CDCl}_3$ ):  $\delta$  (ppm) = 161.2, 148.8, 146.0, 145.1, 134.7, 131.1, 130.8, 129.0, 67.6, 63.0, 31.9, 29.7, 29.4, 29.3, 25.8, 22.7, 14.1; **ATR-FTIR**:  $\tilde{\nu}$  ( $\text{cm}^{-1}$ ) = 2962, 2931, 2917, 2851, 1733, 1636, 1592, 1470, 1304, 1139, 734.

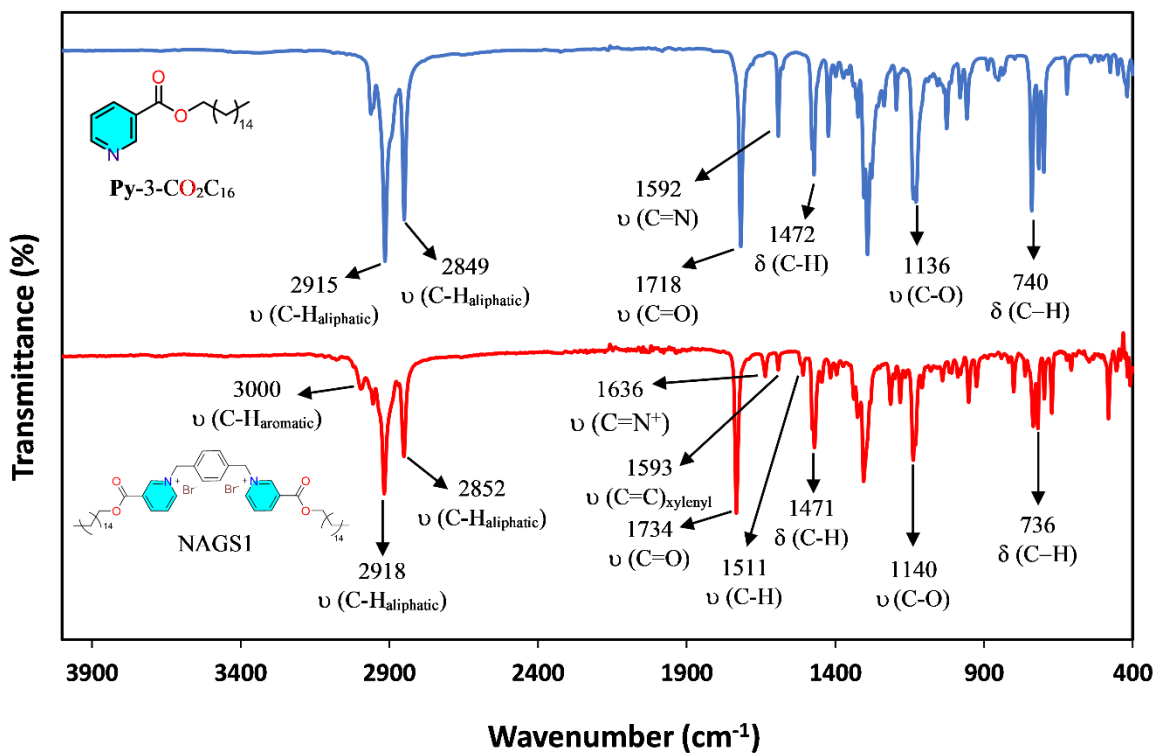


Figure S13. ATR-FTIR spectra of **Py-3-CO<sub>2</sub>C<sub>16</sub>** (blue trace) and **NAGS1** (red trace).

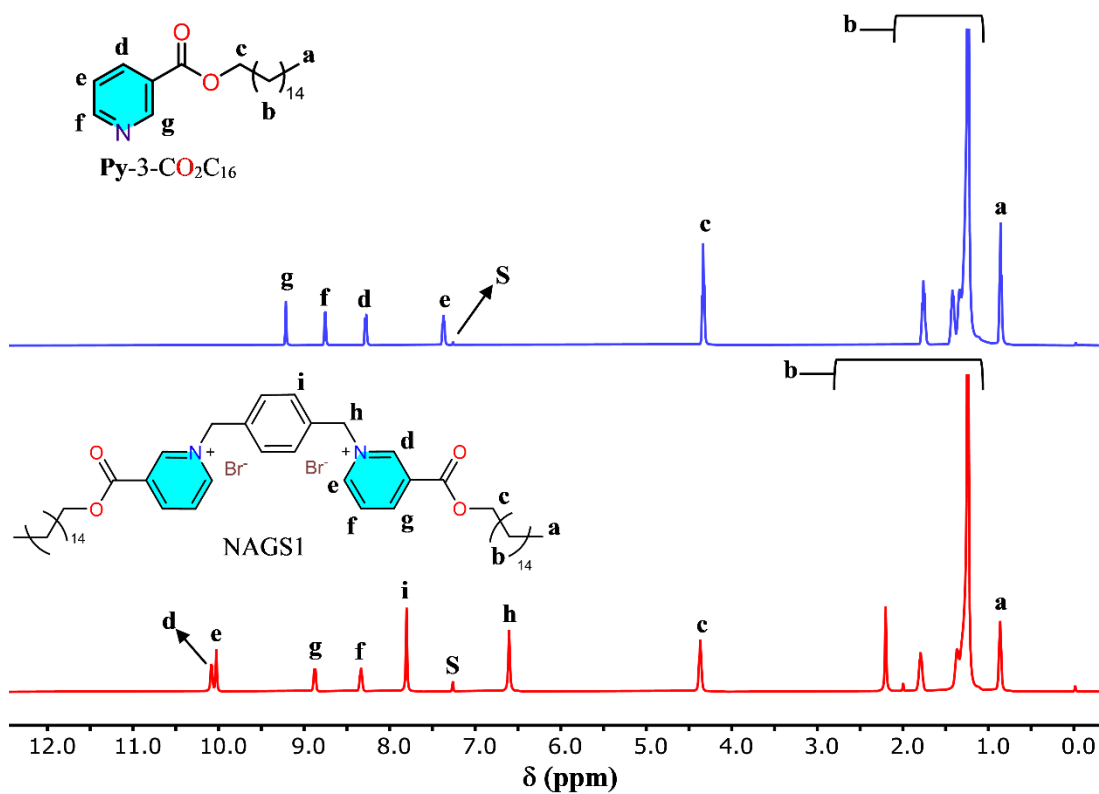
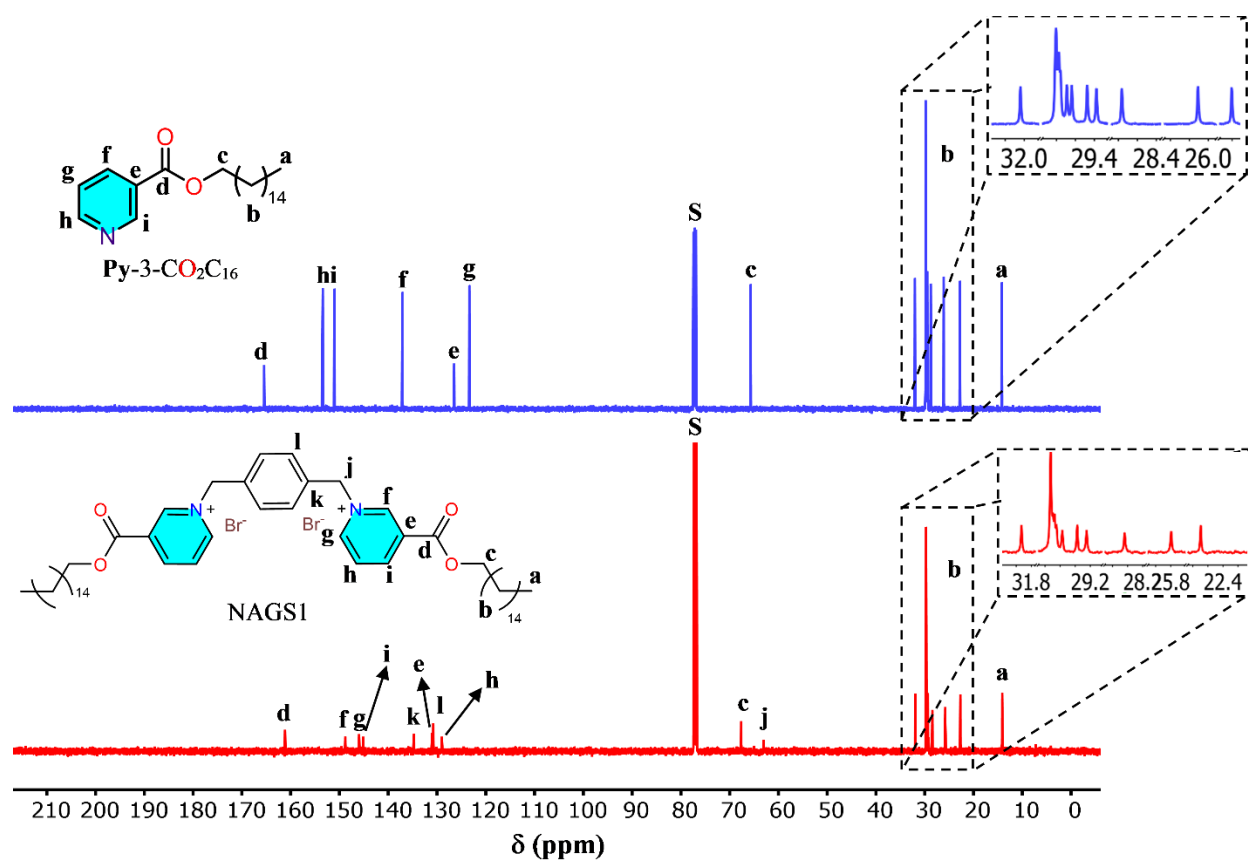


Figure S14. <sup>1</sup>H NMR spectra of **Py-3-CO<sub>2</sub>C<sub>16</sub>** (blue trace) and **NAGS1** (red trace) (S: CDCl<sub>3</sub>).



**Figure S15.**  $^{13}\text{C}$  NMR spectra of  $\text{Py-3-CO}_2\text{C}_{16}$  (blue trace) and NAGS1 (red trace) (S:  $\text{CDCl}_3$ ).

For INAGS, m.p. (corrected) = 231 °C.  $^1\text{H}$  NMR (500 MHz,  $\text{CDCl}_3$ ):  $\delta$  (ppm) = 10.15 (4 H, d), 8.45 (4 H, d), 7.87 (4 H, d), 6.65 (4 H, s), 4.42 (4 H, t), 1.77 (4 H, p), 1.64 (4 H, p), 1.37 (4 H, p), 1.28 (48 H, m), 0.86 (6 H, t);  $^{13}\text{C}$  NMR (125 MHz,  $\text{CDCl}_3/\text{CD}_3\text{OD}$  (1:1)):  $\delta$  (ppm) = 161.7, 146.8, 145.6, 134.6, 131.2, 128.3, 68.2, 64.5, 32.1, 30.1, 29.7, 29.4, 27.4, 26.0, 22.9, 14.2; **ATR-FTIR**:  $\tilde{\nu}$  ( $\text{cm}^{-1}$ ) = 3030, 2956, 2850, 1728, 1640, 1571, 1464, 1274, 1121, 751.

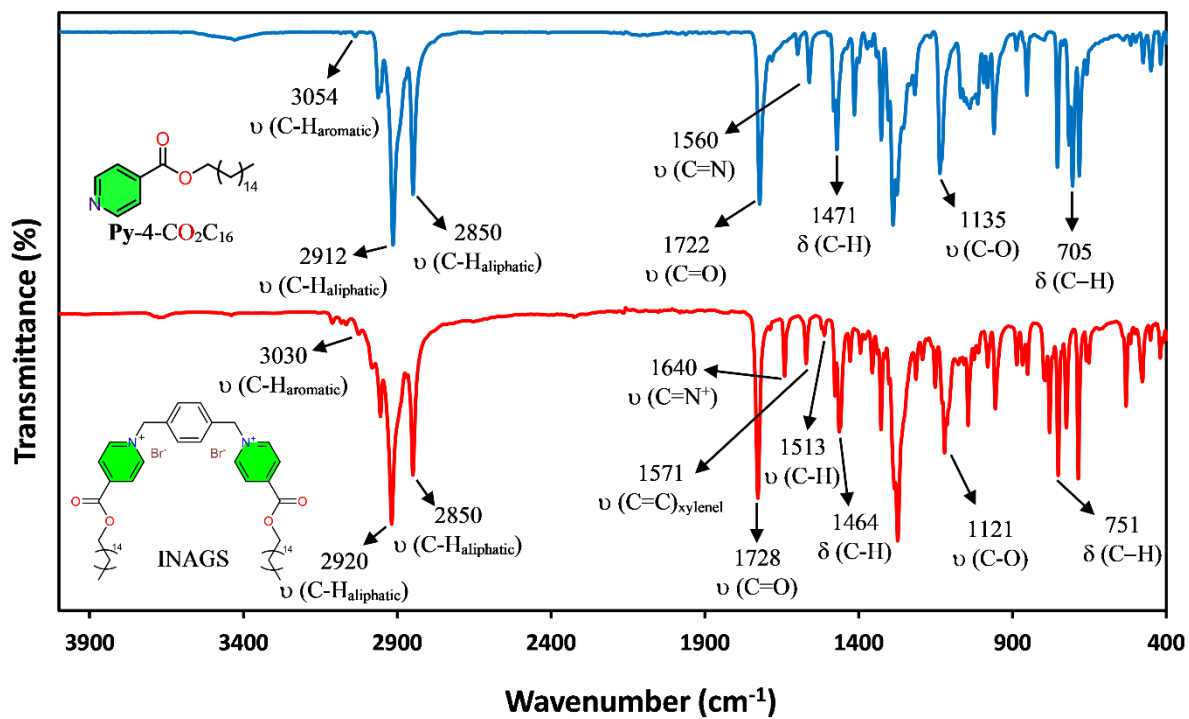


Figure S16. ATR-FTIR spectra of Py-4-CO<sub>2</sub>C<sub>16</sub> (blue trace) and INAGS (red trace).

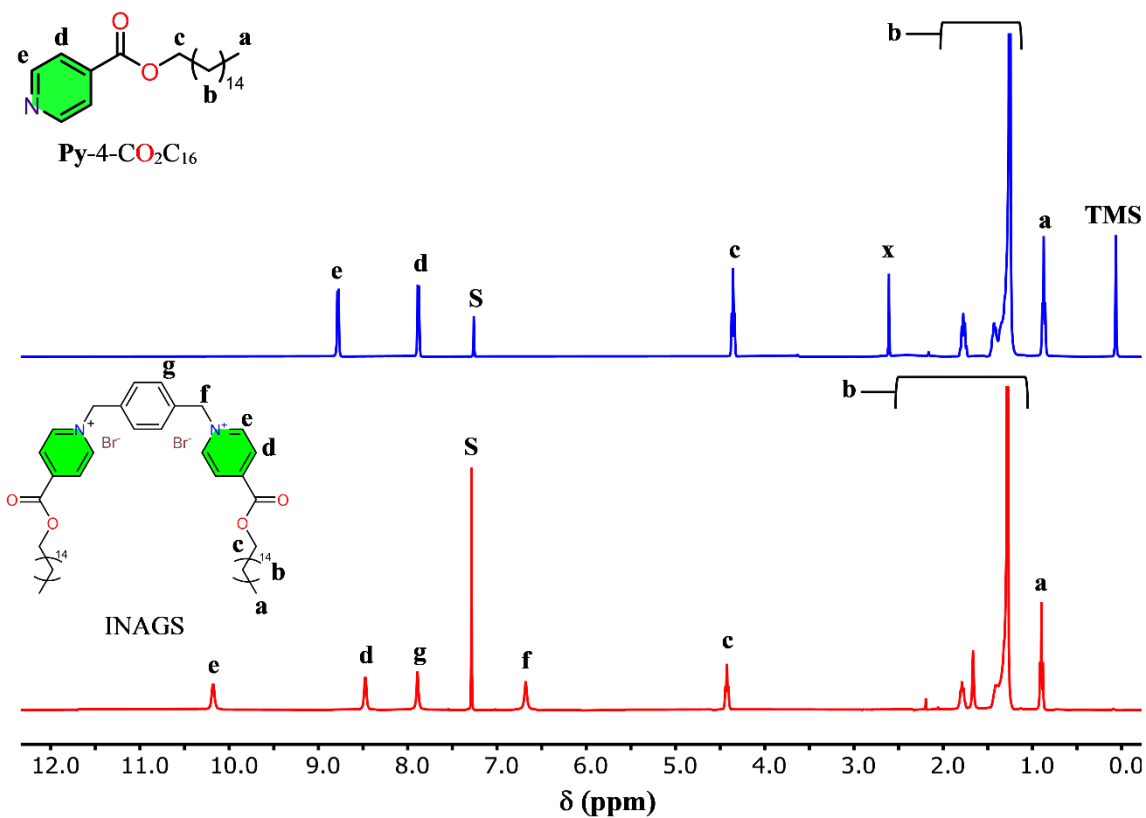
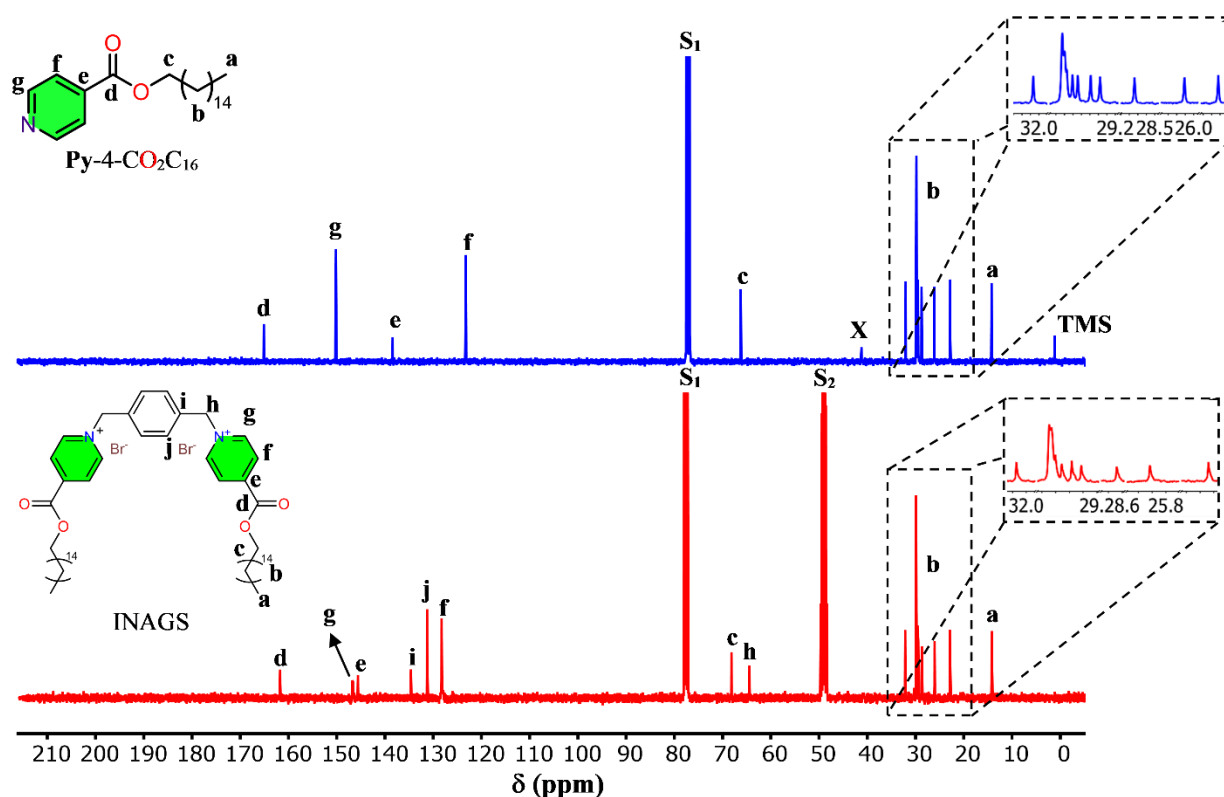


Figure S17. <sup>1</sup>H NMR spectra of Py-4-CO<sub>2</sub>C<sub>16</sub> (blue trace) and INAGS (red trace) (S: CDCl<sub>3</sub>, X: DMSO)



**Figure S18.**  $^{13}\text{C}$  NMR spectra of Py-4-CO<sub>2</sub>C<sub>16</sub> (blue trace) and INAGS (red trace) (S<sub>1</sub>: CDCl<sub>3</sub>, S<sub>2</sub>: CD<sub>3</sub>OD, X: DMSO).

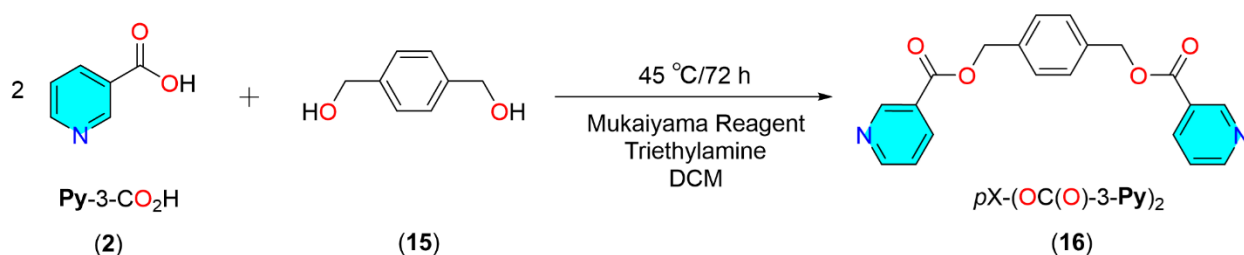
## 3.2 Pyridinium-Based Ester-Bonded Core GS (NAGS2)

### 3.2.1 Synthesis of *p*X-(OC(O)-3-Py)<sub>2</sub>, (1,4-phenylenebis(methylene) dinicotinate, 16)

As shown in **Scheme S4**, the ester appended pyridine of surfactant **16** was synthesized under nitrogen atmosphere in a two-neck round-bottom flask, equipped with a reflux condenser and a rubber septum, charged with a Mukaiyama reagent (2-chloro-1-methylpyridinium iodide) (2.49 g, 2.4 eq.) dissolved in a 180 mL of freshly distilled DCM. Moreover, a mixture of 1,4-benzenedimethanol (**15**, 1 eq.), nicotinic acid (**2**, 2 eq.), and triethylamine (2.7 mL, 4.8 eq.) in 60 mL of DCM was added to the Mukaiyama solution *via* a syringe at RT. The reaction mixture was refluxed for 72 h at 45 °C. Then, the workup included addition of water (2 × 50 mL) to extract side

products and unreacted starting materials, and the organic layer was dried using sodium sulfate. Afterward, the solvent was evaporated to get the desired product with a yield of 68%. Further purification of the product upon recrystallization from hot ethanol was performed to obtain orange needle crystals.

M.p. (corrected) = 145 °C.  $^1\text{H NMR}$  (500 MHz,  $\text{CDCl}_3$ ):  $\delta$  (ppm) = 9.14 (2 H, s), 8.67 (2 H, d), 8.21 (2 H, d), 7.38 (4 H, s), 7.28 (2 H, dd), 5.30 (4 H, s);  $^{13}\text{C NMR}$  (125 MHz,  $\text{CDCl}_3$ ):  $\delta$  (ppm) = 165.1, 153.6, 151.0, 137.2, 135.9, 128.7, 126.0, 123.4, 66.7. **ATR-FTIR**:  $\tilde{\nu}$  ( $\text{cm}^{-1}$ ) = 2974, 1715, 1650, 1589, 1717, 1024, 739. **Elemental analysis** ( $\text{C}_{20}\text{H}_{16}\text{N}_2\text{O}_4$ ); calculated (%) C, 68.96; H, 4.63; N, 8.04; found (%) C, 68.87; H, 4.68; N, 7.83,



**Scheme S4.** The synthesis of **(16)**  $p\text{X}-(\text{OC}(\text{O})\text{-3-Py})_2$

Precursor **16** was examined using ATR-FTIR (**Figure S19**, **green trace**), a characteristic peak corresponding to the carbonyl ( $\text{C}=\text{O}$ ) stretching frequency was shifted from 1700 to 1715  $\text{cm}^{-1}$  upon esterification. As compared to **Py-3-CO<sub>2</sub>H** (**Figure S19**, **blue trace**), it was accompanied with another shift in the stretching vibration of  $\text{C}=\text{N}$  from 1596 to 1650  $\text{cm}^{-1}$ . For  $^1\text{H}$  and  $^{13}\text{C}$  NMR, a methylene moiety was evidenced upon shifting from 4.48 to 5.30 ppm as well as 62.8 to 66.7 ppm (**Figure S20** and **Figure S21**, **green trace**).<sup>4</sup>



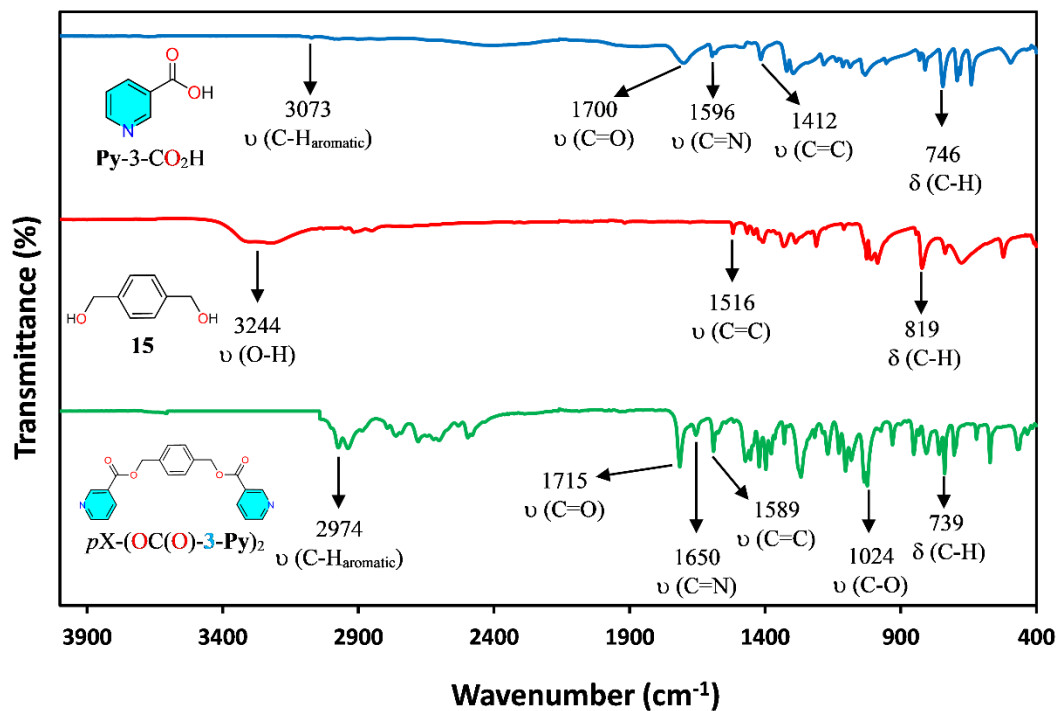


**Figure S19.** ATR-FTIR spectra of Py-3-CO<sub>2</sub>H (2, blue trace), 15 (red trace), and pX-(OC(O)-3-Py)<sub>2</sub> (16, green trace)

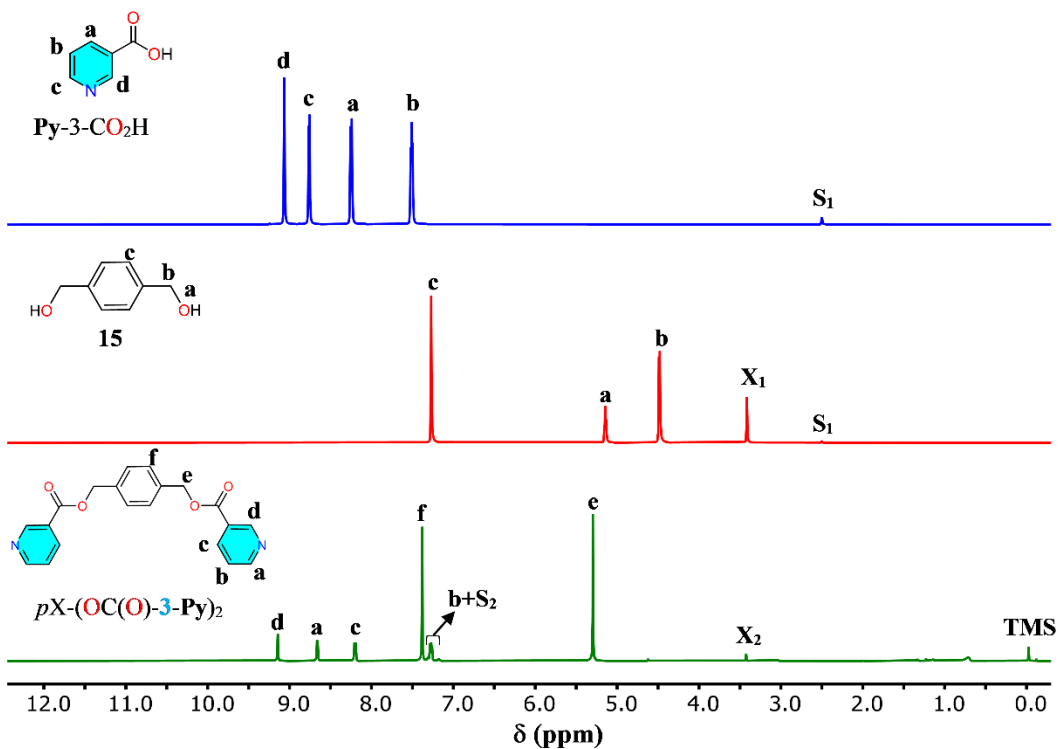


**Figure S20.** <sup>1</sup>H NMR spectra of Py-3-CO<sub>2</sub>H (2, blue trace), 15 (red trace), and pX-(OC(O)-3-Py)<sub>2</sub> (16, green trace) (S<sub>1</sub>: DMSO-*d*<sub>6</sub>, S<sub>2</sub>: CDCl<sub>3</sub>, X<sub>1</sub>: H<sub>2</sub>O, X<sub>2</sub>: EtOH).

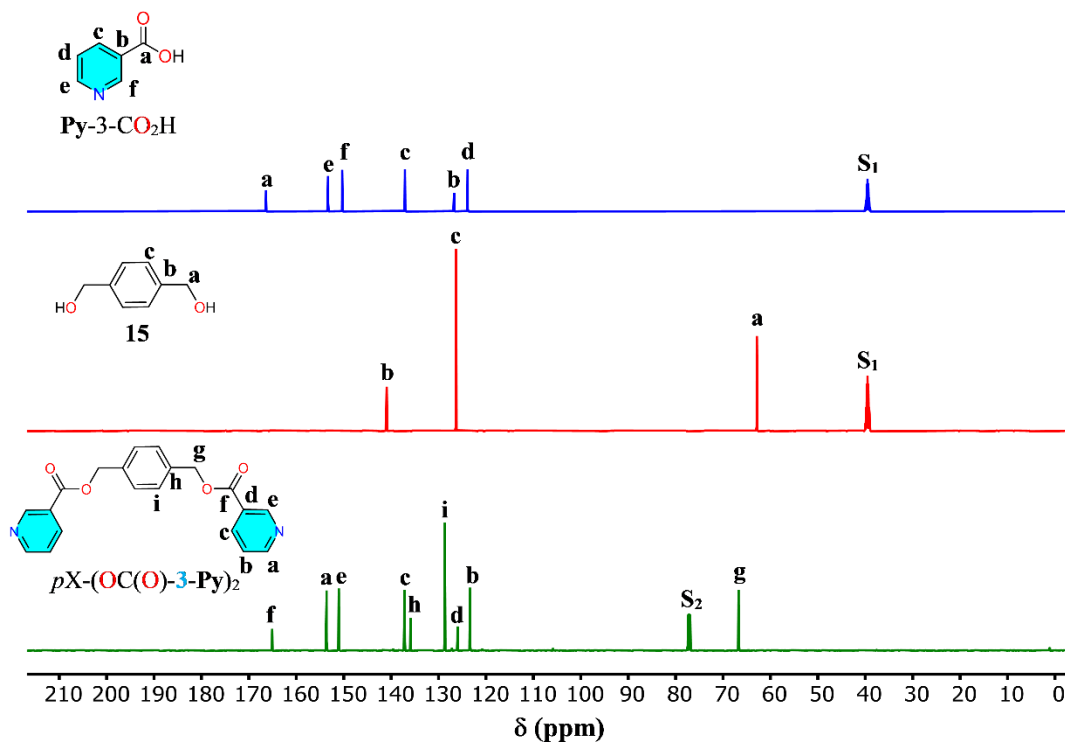


**Figure S21.**  $^{13}\text{C}$  NMR spectra of **Py-3-CO<sub>2</sub>H** (**2**, blue trace), **15** (red trace), and  $p\text{X}-(\text{OC}(\text{O})-3\text{-Py})_2$  (**16**, green trace) ( $\text{S}_1$ :  $\text{DMSO-}d_6$ ,  $\text{S}_2$ :  $\text{CDCl}_3$ ).

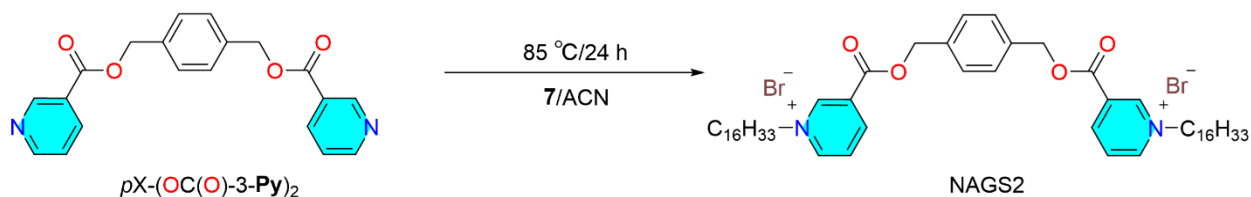
### 3.2.2 Synthesis of NAGS2 (3,3'-(((1,4-phenylenebis

#### (methylene))bis(oxy))bis(carbonyl))bis(1-hexadecylpyridin-1-ium)•2Br

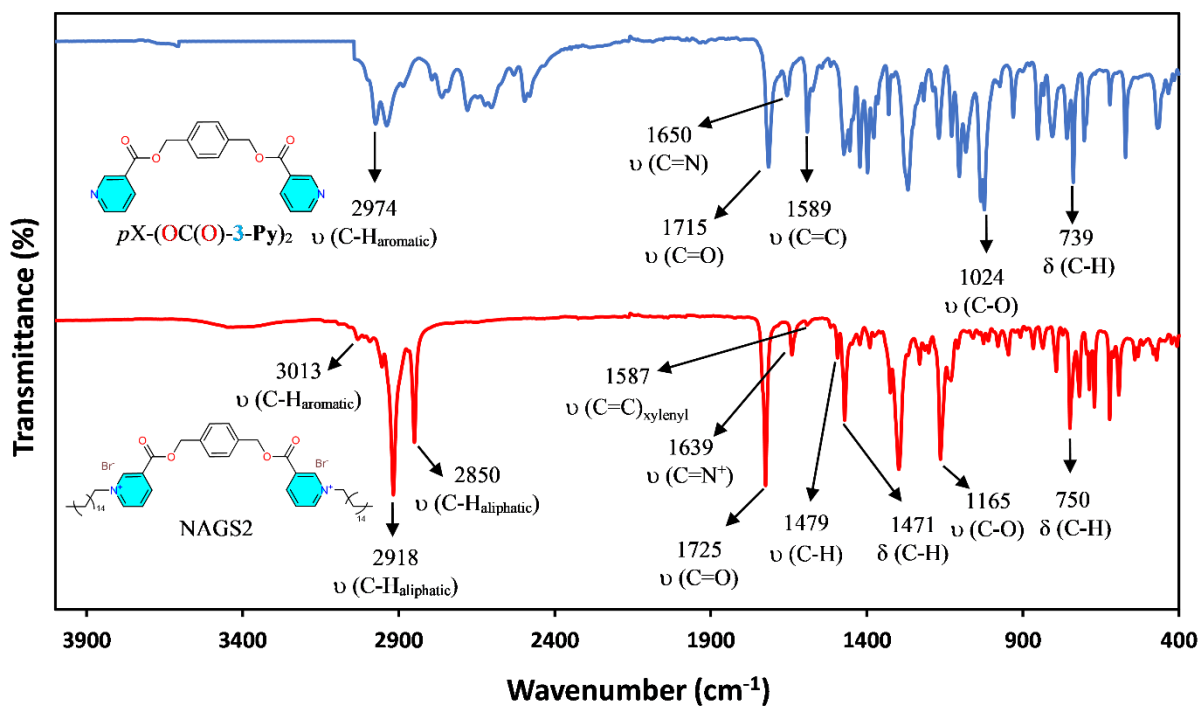
In a round-bottom flask equipped with a reflux condenser capped with a rubber septum charged with a solution of  $p\text{X}-(\text{OC}(\text{O})-3\text{-Py})_2$  (**16**, 0.5 g, 1 eq.) in 15 mL hot ACN together with 4 mL toluene solution of 1-bromohexadecane (**7**, 2 eq., **Scheme S5**). The reaction mixture was refluxed for 24 h at 85 °C. The product was collected using suction filtration, then recrystallized using hot chloroform/diethyl ether to yield a white solid then washed with 20 mL of ethanol and dried over air with a yield of 77%.

M.p. (corrected) = 187 °C.  $^1\text{H}$  NMR (500 MHz,  $\text{CD}_3\text{OD}$ ):  $\delta$  (ppm) = 9.70 (2 H, s), 9.28 (2 H, d), 9.12 (2 H, d), 8.33 (2 H, t), 7.72 (4 H, s), 6.06 (2 H, s), 4.52 (4 H, t), 2.20 (4 H, p), 1.86 (4 H, p), 1.57 (4 H, p), 1.34 (44 H, m), 0.93 (6 H, t);  $^{13}\text{C}$  NMR (125 MHz,  $\text{CD}_3\text{OD}$ ):  $\delta$  (ppm) = 162.2, 148.5,

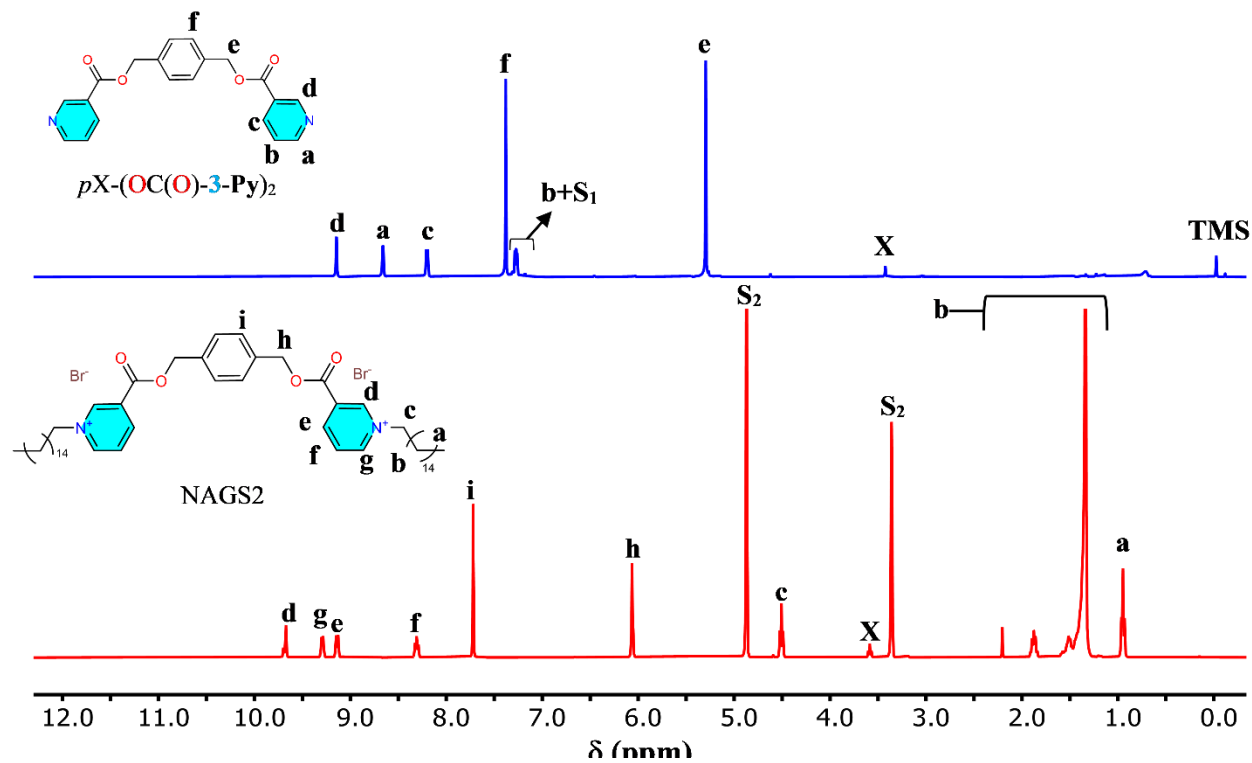
146.8, 135.7, 132.5, 132.3, 131.1, 129.6, 68.0, 64.9, 33.3, 32.6, 30.3, 30.3, 30.2, 30.2, 30.0, 30.0  
 29.2, 26.5, 23.3, 14.0. **ATR-FTIR**  $\tilde{\nu}$  (cm<sup>-1</sup>) = 3013, 2934, 2840, 1725, 1639, 1471, 1972, 1165,  
 750.



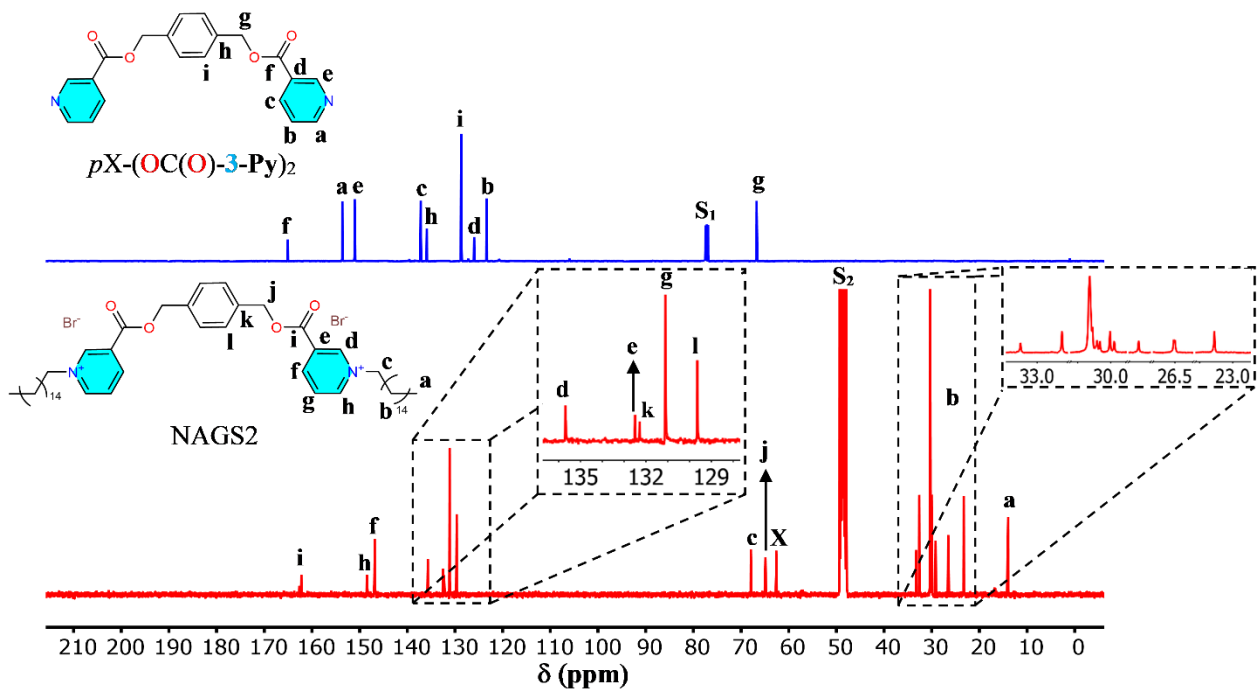
ATR-FTIR (**Figure S22**, red trace) confirmed the structure of **17** with a blue shift of the C=N peak from 1650 to 1639 cm<sup>-1</sup>. The latter was further accompanied with emergence of stretching bands for C-H<sub>aliphatic</sub> in the region of 2918-2850 cm<sup>-1</sup>. In addition, a red shift for the carbonyl (C=O) peak centered at 1715 up to 1725 cm<sup>-1</sup>. The alkylation was further evidenced upon the resemblance of a peak corresponding to the methylene moiety closest to the pyridine ring at 4.52 and 67.9 ppm as shown in <sup>1</sup>H and <sup>13</sup>C NMR, respectively (**Figure S23** and **Figure S24**, red traces).



**Figure S22.** ATR-FTIR spectra of *pX*-(OC(O)-3-Py)<sub>2</sub> (**16**, blue trace), and NAGS2 (**15**, red trace).



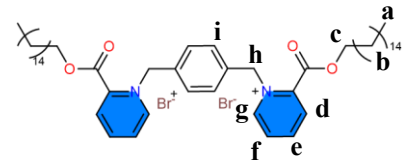
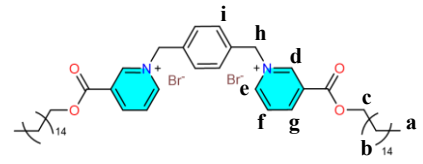
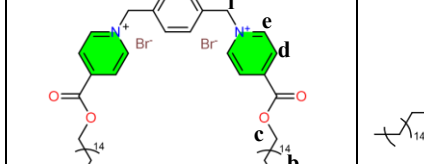
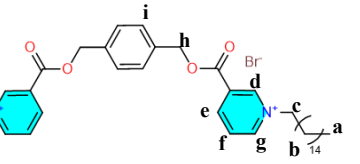
**Figure S23.**  $^1\text{H}$  NMR spectra of  $p\text{X}-(\text{OC}(\text{O})-3\text{-Py})_2$  (16, blue trace), and NAGS2 (15, red trace) (S<sub>1</sub>:  $\text{CDCl}_3$ , S<sub>2</sub>:  $\text{CD}_3\text{OD}$ , X: EtOH).



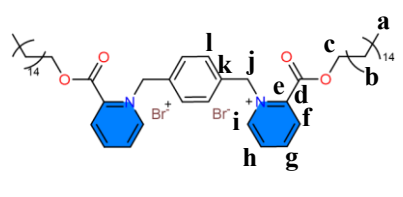
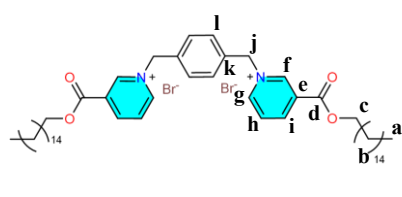
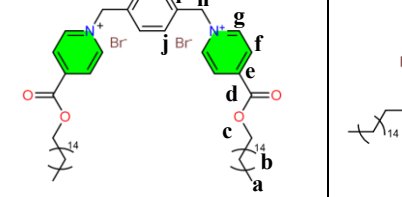
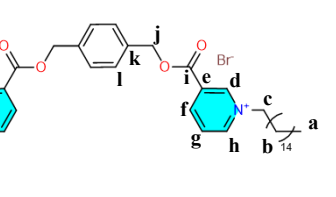
**Figure S24.**  $^{13}\text{C}$  NMR spectra of  $p\text{X}-(\text{OC}(\text{O})-3\text{-Py})_2$  (16, blue trace), and NAGS2 (15, red trace) (S<sub>1</sub>:  $\text{CDCl}_3$ , S<sub>2</sub>:  $\text{CD}_3\text{OD}$ , X: EtOH).

## 4. Summary of Spectral Data

**Table S1.**  $^1\text{H}$  NMR chemical shifts ( $\delta$ , ppm) of the synthesized GSs.

	<i>PAGS</i>	<i>NAGS1</i>	<i>INAGS</i>	<i>NAGS2</i>
				
<i>H-a</i>	0.87	0.88	0.86	0.93
<i>H-b</i>	1.25-2.13	1.24-2.20	1.28-1.77	1.34-2.20
<i>H-c</i>	4.39	4.38	4.42	4.52
<i>H-d</i>	10.11	10.09	8.45	9.70
<i>H-e</i>	8.88	10.02	10.15	9.12
<i>H-f</i>	8.32	8.87	6.65	8.33
<i>H-g</i>	10.00	8.35	7.87	9.28
<i>H-h</i>	6.61	7.80		6.06
<i>H-i</i>	7.80	6.60		7.72

**Table S2.**  $^{13}\text{C}$  NMR chemical shifts ( $\delta$ , ppm) of the synthesized GSs.

	<i>PAGS</i>	<i>NAGS1</i>	<i>INAGS</i>	<i>NAGS2</i>
				
<i>C-a</i>	14.2	14.1	14.2	14.0
<i>C-b</i>	32.1-22.8	31.9-22.7	32.1-22.9	33.3-23.3
<i>C-c</i>	67.9	67.6	68.2	68.0
<i>C-d</i>	161.3	161.2	161.7	135.7
<i>C-e</i>	145.3	131.1	145.6	132.5
<i>C-f</i>	131.0	148.8	128.3	146.8
<i>C-g</i>	149.1	146.0	146.8	131.1
<i>C-h</i>	134.9	129.0	64.5	148.5
<i>C-i</i>	146.2	145.1	134.6	162.2
<i>C-j</i>	63.3	63.0	131.2	64.9
<i>C-k</i>	131.4	134.7		132.3
<i>C-l</i>	129.2	130.8		129.6

**Table S3.** ATR-FTIR wavenumbers ( $\tilde{\nu}$ ,  $\text{cm}^{-1}$ ) of the synthesized GSs.

	<i>PAGS</i>	<i>NAGS1</i>	<i>INAGS</i>	<i>NAGS2</i>
$\tilde{\nu}$ (C-H <sub>aromatic</sub> )	2999	3000	3030	3013
$\tilde{\nu}$ (C-H <sub>aliphatic</sub> )	2920, 2851	2918, 2852	2920, 2850	2918, 2850
$\tilde{\nu}$ (C=N <sup>+</sup> )	1640	1636	1640	1587
$\tilde{\nu}$ (C=C) <sub>xylene</sub>	1594	1593	1571	1587
$\tilde{\nu}$ (C=O)	1725	1734	1728	1725
$\tilde{\nu}$ (C-H)	1497	1511	1513	1479

## 5. References

1. A. F. Eftaiha, A. K. Qaroush, A. S. Abo-shunnar, S. B. Hammad, K. I. Assaf, F. M. Al-Qaisi and M. F. Paige, *Langmuir*, 2022, **38**, 8524–8533.
2. D. Bora, B. Deb, A. L. Fuller, A. M. Z. Slawin, J. Derek Woollins and D. K. Dutta, *Inorganica Chimica Acta*, 2010, **363**, 1539–1546.
3. P. Scrimin, P. Tecilla and U. Tonellato, *J. Org. Chem.*, 1994, **59**, 18–24.
4. K. Suzuki, H. Kitagawa and T. Mukaiyama, *BCSJ*, 1993, **66**, 3729–3734.